Nanoscale

REVIEW

View Article Online
View Journal | View Issue

Cite this: *Nanoscale*, 2024, **16**, 16344

Recent advances on applications of single-walled carbon nanotubes as cutting-edge optical nanosensors for biosensing technologies

Hannah M. Dewey, Ashley Lamb and Januka Budhathoki-Uprety *

Single-walled carbon nanotubes (SWCNTs) possess outstanding photophysical properties which has garnered interest towards utilizing these materials for biosensing and imaging applications. The near-infrared (NIR) fluorescence within the tissue transparent region along with their photostability and sizes in the nanoscale make SWCNTs valued candidates for the development of optical sensors. In this review, we discuss recent advances in the development and the applications of SWCNT-based nano-biosensors. An overview of SWCNT's structural and photophysical properties, sensor development, and sensing mechanisms are described. Examples of SWCNT-based optical nanosensors for detection of disease biomarkers, pathogens (bacteria and viruses), plant stressors, and environmental contaminants including heavy metals and disinfectants are provided. Molecular detection in biofluids, *in vitro*, and *in vivo* (small animal models and plants) are highlighted, and sensor integration into portable substrates for implantable and wearable sensing devices has been discussed. Recent advancements, which include high throughput assays and the use of machine learning models to predict more sensitive and robust sensing outcomes are discussed. Current limitations and future perspectives on translation of SWCNT optical probes into clinical practices have been provided.

Received 2nd May 2024,
Accepted 9th August 2024

DOI: 10.1039/d4nr01892c

rsc.li/nanoscale

Introduction

The need to detect specific molecules has become an increasing demand in healthcare, clinical medicine, food safety, environmental monitoring, and homeland security.[1] Early

Department of Textile Engineering, Chemistry and Science, Wilson College of Textiles, North Carolina State University, Raleigh, NC, 27695, USA.
E-mail: jbudhat@ncsu.edu

Hannah Dewey

Hannah Dewey received her Ph.D. degree in Fiber and Polymer Science from North Carolina State University in 2024 under the guidance of Dr Januka Budhathoki-Uprety. Her dissertation research focused on developing optical nanosensors using single-walled carbon nanotubes for the detection of biological indicators and emerging contaminants. She has won several awards in poster and oral research presentation competitions. She has been accepted to the Carolina Cancer Nanotechnology Training Program as a T32 Postdoctoral Fellow where she will research new technologies for cancer diagnosis and treatment.

Ashley Lamb

Ashley Lamb received her B.S. in Polymer & Color Chemistry and B.S. in Human Biology in 2024 from North Carolina State University. She was awarded Centennial Scholarship while attending NC State University. She is currently studying at the University of North Carolina School of Medicine. During her undergraduate years, Ashley worked in the Budhathoki-Uprety lab and conducted her research in biomedical applications of carbon nanotubes as potential nanosensors for detection of various analytes.

detection of diseases, health hazards, toxins in aquatic and terrestrial environments, and stresses in agricultural crops can help facilitate early treatment, mitigate life-threatening effects, and preserve aquatic and terrestrial organisms. Nanomaterials provide unique opportunities to develop tunable molecular probes for the detection of analytes due to their outstanding optical, electrical, and magnetic properties.[1–3] Among such nanomaterials are single-walled carbon nanotubes (SWCNTs) which possess exceptional optical, photothermal, and electrical properties.[4,5] Seminal works from the Smalley and Weisman research groups on SWCNT structure and their photophysical properties which include the discovery on SWCNT band-gap fluorescence,[6,7] unique spectral characteristics based on their structure,[8] and their sensitivity to environmental changes[9] led to an increasing interest in SWCNTs for their applications as molecular sensors and imaging agents. In addition, SWCNTs offer the following advantages: (1) high sensitivity due to high surface area-to-volume ratio; (2) non-photo bleaching fluorescence in the near-infrared spectral window; (3) fast response time; (4) lower potential of redox reaction and surface fouling effects; (5) high stability and longer lifetime.[1,3] SWCNTs have many attributes that are ideal for *in vitro* and *in vivo* optical sensing. SWCNTs are highly photostable and exhibit sustained emission under intense light irradiation unlike small molecule organic fluorophores which undergo rapid photobleaching.[5,10,11] SWCNTs emit within the NIR region (900–1600 nm) where light scattering and autofluorescence from biological tissue are negligible.[5,10] Furthermore, SWCNTs are inherently thermally stable, have long shelf-life, and stable when subjected to body temperatures for longer periods of time without affecting their physical, chemical, or optical properties; unlike common small molecule fluorophores and electrochemical sensors.[11,12] SWCNTs, can occur as many distinct species (33 different (n, m) species) with unique photophysical characteristics,[7] making these materials suitable for multiplexed sensing, overcoming the challenges associated with small molecule optical and electrochemical sensors.[5,10–13]

This review focuses on the recent advances in applications of single-walled carbon nanotube-based optical sensors in the biological and environmental sectors. Several examples of nanosensors for detection of various classes of analytes such as hormones, proteins, cancer biomarkers, nucleic acids, pathogens, and neurotransmitters in biofluids, *in vitro* and *in vivo* are discussed. The review highlights how incorporation of nanosensors into polymeric matrixes results in various platforms for portable, implantable, and wearable sensing applications. An overview of SWCNT structure, optical properties, and sensing mechanisms are discussed. Furthermore, we evaluate the status of SWCNT-based sensor applications, discuss current challenges and provide recommendations for future sensor developments. The findings from this review will provide a pathway for further improvements and advancements in engineering efficient optical probes and sensors.

Januka Budhathoki-Uprety

Januka Budhathoki-Uprety received her PhD degree in Chemistry in 2012 from North Carolina State University, USA, under the supervision of Prof. Bruce Novak. She obtained her MS degree in Chemistry from Western Carolina University, USA; B.Sc. and M.Sc. degrees from Tribhuvan University, Nepal. She worked as a postdoctoral fellow at Memorial Sloan Kettering Cancer Center, NY. She is currently an Assistant Professor at NC State University. She is recipient of the NC State Outstanding Teacher Award 2023–2024 and a member of the Academy of Outstanding Teachers. Her current research focuses on polymer chemistry, nanotechnology and developing molecular sensors.

Structure of single-walled carbon nanotubes (SWCNTs)

Single-walled carbon nanotubes (SWCNTs) consist of sp^2 hybridized carbon atoms that can be considered as rolling of a single layer of graphene sheets into hollow cylindrical tubes with diameters ranging from 0.48 to 2.0 nm (ref. 8) and roll-up angles and (n, m) integers describe the nanotube's circumference (Fig. 1a).[5] Based on roll-up angles, SWCNTs can be chiral.[5] The chirality of a nanotube can be described by $C_h = na_1 + ma_2$, where the nanotube is rolled-up along the vector C_h and $|a_1| = |a_2| \equiv a = \sqrt{3}a_{C-C}$ with the carbon–carbon bond length equaling 0.144 nm.[2,5] Chiral SWCNT structures have roll-up angles between 0° and 30°. SWCNT structures with roll-up angles of 0° and $m = 0$ are "zigzag" structures, and those with roll-up angles of 30° and $m = n$ are "armchair" structures.[5] The chirality of a nanotube can be used to describe characteristics such as circumference, diameter, roll-up angle, and electronic structure. The circumference can be calculated by the following equation:

$$|C_h| = a\sqrt{n^2 + nm + m^2}$$

The diameter would then be $|C_h|/\pi$, and the roll-up angle (α) would be the following:

$$\alpha = \tan^{-1}\left(\frac{\sqrt{3}m}{2n + m}\right).$$

Furthermore, the integers (n, m) can indicate whether a nanotube is metallic, semi-metallic, or semiconducting by taking the difference of $n - m$. If that difference is equal to 0 ($n = m$), the nanotube will have no energy band gap thereby giving it metallic properties. Additionally, if $n \neq m$ and the

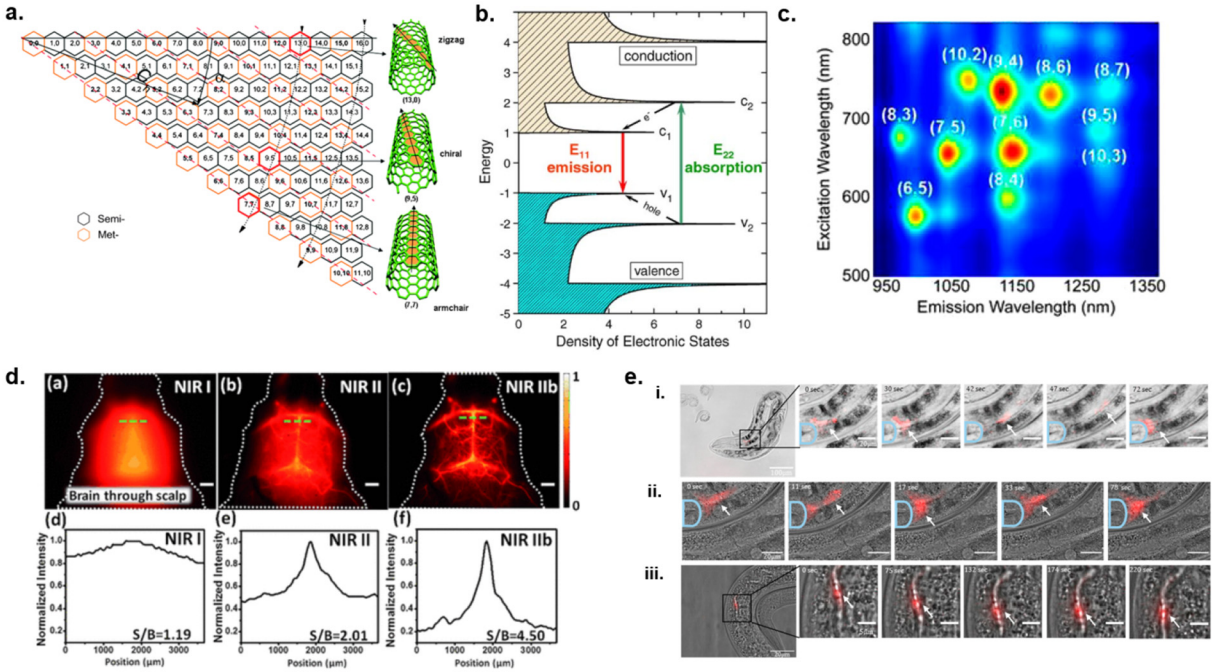

Fig. 1 Structure and optical properties of single-walled carbon nanotubes. (a) Scheme of SWCNT construction. The roll-up vector will become the circumference of the nanotube known as C_h and is denoted as (n, m).[166] (b) Diagram of electronic states for semi-conducting SWCNTs.[167] Reprinted with permission from ref. 167. Copyright 2004 Springer Nature. (c) Photoluminescence excitation/emission map of semi-conducting SWCNTs of various charities.[168] Reprinted with permission from ref. 168. Copyright 2017 American Chemical Society. (d) Through skull NIR fluorescence spectral imaging of SWCNTs in mouse brain without craniotomy, (a–c) images and (d–f) spectra.[18] Reprinted with permission from ref. 18. Copyright 2015 John Wiley and Sons (e) *In vivo* NIR fluorescence imaging of ssDNA–SWCNTs (red) within nematodes. SWCNTs were tracked moving from the pharyngeal valve to the intestine (i and ii) and moving through the intestinal tract (iii) over time.[20] Reprinted with permission from ref. 20. Copyright 2021 Elsevier.

difference is divisible by 3, then the nanotube will have a small band gap and exhibit semi-metallic properties.[2,5] On the other hand, if $n - m = 1$ or 2 then the nanotubes will have a large sized band-gap resulting in semiconducting properties.

Photoluminescence of single-walled carbon nanotubes

Semiconducting nanotubes can absorb visible or near-infrared light and emit near-infrared fluorescence (900 nm–1600 nm).[2,4,5] Once a nanotube absorbs a photon, an electron–hole pair which is also known as an exciton is generated.[8] Excitons diffuse between 100 nm and 200 nm along the SWCNTs axis.[14,15] Radiative recombination of electron–hole (e^-h^+) pair induces fluorescence emission in the NIR region.[9,16] Fig. 1b illustrates a semiconducting SWCNT's density of electronic states, electronic transitions can occur at E_{11} (short-wave infrared region), E_{22} (visible wavelengths), and E_{33} (violet or near-ultraviolet region) where an electron is excited from the valence band to its corresponding conduction band. Electronic transition from (v_2) to (c_2) results in E_{22} absorption. The electron will rapidly relax non-radiatively until it reaches the bottom of the conduction band and the hole reaches the top of the valence band.[5] Emission takes place through the competing radiative decay channel while the electron–hole pair slowly recombines from the conduction band back to its corresponding valence band as an E_{11} transition (c_1 to v_1).[2,5] The absorption of light at a shorter wavelength and the radiative relaxation of an electron (E_{11}, E_{22}, E_{33}) from the excited state back to the resting state at longer wavelengths is known as photoluminescence (*i.e.*, fluorescence) which occurs in the NIR region. Each (n, m) chirality has a specific band-gap where excitation and emission occur at characteristic wavelengths.[2,4,5] By analyzing these spectral wavelengths *via* fluorescence and Raman spectroscopies, a relationship between chiral index (n,m)/diameter and band-gap was established.[2,5,8] Furthermore, photoluminescence excitation–emission maps are constructed where the intensity of emission is plotted against excitation *vs.* emission wavelengths in the form of a surface map (Fig. 1c) which is used in the analysis of SWCNT samples.[5,17]

One of the major advantages of photoluminescent SWCNTs includes highly photostable emissions in the NIR range. This NIR spectral window is where autofluorescence from biomolecules in tissues and biofluids are negligible. Diao *et al.* and Hong *et al.* utilized this characteristic of SWCNTs for through skull imaging of mouse brain and its cerebro-vasculature without need for a craniotomy (Fig. 1d).[18,19] These studies demonstrated imaging in the NIR II window (1000 nm–

1700 nm) at a depth >2 mm in mouse brain for blood perfusion.[18,19] The resolved vasculature imaging along with the increased signal-to-background ratios (SBRs) for NIR spectra (Fig. 1d) demonstrate clear potential for SWCNTs based probes in *in vivo* bioimaging.

In regard to photostability, the quantum yields remain stable under ambient conditions over long periods of photoexcitation.[5] Furthermore, SWCNTs are less prone to blinking (random switching between bright and dark states) under continuous light irradiation as opposed to inorganic quantum dots.[5] Hendler-Neumark *et al.* utilized non-photobleaching nature of photostable SWCNTs to study digestive system of *C. elegans* nematode.[20] NIR fluorescence imaging *in vivo* showed that the SWCNTs were eaten by the worms. Tracking of the SWCNTs *in vivo* showed their movements from the pharyngeal valve through the intestine over time (Fig. 1e). The results from this study show a high potential for using SWCNTs imaging agents for the study of biological processes.

Although SWCNT-based materials provide a great opportunity for development of optical probes, imaging agents, and sensors, SWCNTs require functionalization for such applications. Pristine SWCNTs are strongly hydrophobic and occur in bundles due to their strong hydrophobic (van der Waals) forces.[2,5,21] Within these bundles, irreversible energy transfer takes place from excited semiconducting SWCNTs to metallic SWCNTs, resulting in quenching of nanotube fluorescence.[2,5] Furthermore, bundled nanotubes are insoluble in common aqueous and organic solvents and are not biocompatible.[22] Therefore, functionalization of the nanotube surface is needed for solubility, biocompatibility, and photophysical characteristics.[2,23,24]

Surface functionalization

SWCNTs can be functionalized by covalent and non-covalent methods to render nanotubes dispersed into aqueous and organic solvents.[2,21,25] Covalent functionalization can occur *via* oxidation, halogenation, 1,3-dipolar cycloaddition *etc.* of carbon–carbon double bonds on the nanotube surface resulting in the formation of carboxylic acid (–COOH) and other functional groups along the surface of nanotubes.[2,26] Although intentional introduction of defect sites appear to retain photophysical characteristics of nanotubes (*vide infra*), a high degree of covalent functionalization could compromise the nanotube's photophysical properties due to disruption on the conjugation along the nanotube surface.[2,21,25]

In non-covalent functionalization, molecules can physically adsorb onto the nanotube surface *via* hydrophobic interactions or π–π stacking of aromatic compounds on graphitic surface of SWCNTs without interrupting the π-conjugated system of nanotubes.[2,22,27] Thus non-covalent functionalization method, which preserves the intrinsic photophysical properties of nanotubes, is widely employed to develop SWCNT-based optical probes, sensors, and imaging agents. The non-covalent method for preparation of NIR photoluminescent nanotube was first reported by O'Connell *et al.* in 2002 in which nanotubes were dispersed in aqueous solution with sodium dodecyl sulfate (SDS), an anionic surfactant, *via* vigorous sonication and centrifugation methods.[6] The sonication method was used to provide sufficient energy to disrupt the van der Waals forces in the bundled nanotubes to allow for individual nanotubes to be dispersed in the surfactant solution.[5,6] Subsequent centrifugation process was applied to remove bundled tubes, carbonaceous impurities, and any residual metal catalysts, leaving a supernatant comprised of de-bundled nanotubes which exhibited NIR fluorescence.[5,6]

The SWCNT suspensions with surfactants such as sodium dodecylbenzenesulfonate (SDBS), sodium dodecylsulfonate (SDS), dodecyltrimethylammonium bromide (DTAB) and cetyltrimethylammonium bromide (CTAB);[28] as well as polymers including polystyrene sulfonate (PSS), and poly(vinylpyrrolidone) (PVP) have been reported.[28,29] The fluorescence of SWCNTs dispersed with SDBS, SDS, and CTAB were also reported.[28] These dispersant compounds are amphiphilic, in which the hydrophobic groups interact with the graphitic surface on nanotubes and the hydrophilic groups render the aqueous solubility. In the case of surfactants, cylindrical or hemimicellar micelles are formed around the nanotubes and the polar head groups provide electrostatic repulsion to prevent re-aggregation of nanotubes in solution. The surfactants could cover the nanotube surface more or less densely[30] (Fig. 2a). Researchers have also reported random adsorption of surfactant molecules onto SWCNT surface.[31] Polymers could wrap tightly around the nanotube as a result of their thermodynamic drive to eliminate the interface between the nanotube and its aqueous medium, while providing electrostatic/steric repulsion with their hydrophilic/bulky functional group (Fig. 2d).[29] Biopolymers, such as DNA (Fig. 2b),[32] phospholipids (Fig. 2c),[33,34] peptides (Fig. 2e),[35,36] and polysaccharides (Fig. 2f),[37] have been used to solubilize SWCNTs through similar mechanisms as previously described. For example, single-stranded DNA (ssDNA) can adsorb onto the nanotube surface through π–π stacking of the DNA bases with graphitic side walls of nanotubes while providing electrostatic repulsion *via* the negatively charged phosphate backbone (Fig. 2b) thereby achieving colloidal stability.[32,38] Furthermore, bovine serum albumin (BSA), amphiphilic peptides, and phospholipids have been shown to form complexes with SWCNTs. These molecules not only provide solubility but can aid in biocompatibility of SWCNTs.

The use of synthetic polymers could diversify SWCNT applications as one could tailor polymer synthesis in order to provide specific functional properties.[39] Studies have shown polyfluorenes,[40,41] polycarbazoles,[42] conjugated polymers such as polyarylene ethylenes,[43] polyethylene glycol (PEG) derivatives,[44] and polycarbodiimides (PCD)[39] as good dispersants for SWCNTs. Some classes of polymer have been noted to selectively disperse SWCNTs based on their diameter and thus have an application for sorting nanotubes of specific chiralities.[40–43] However, other polymers such as PCDs and PEG conjugated with various functional groups have been used to enhance

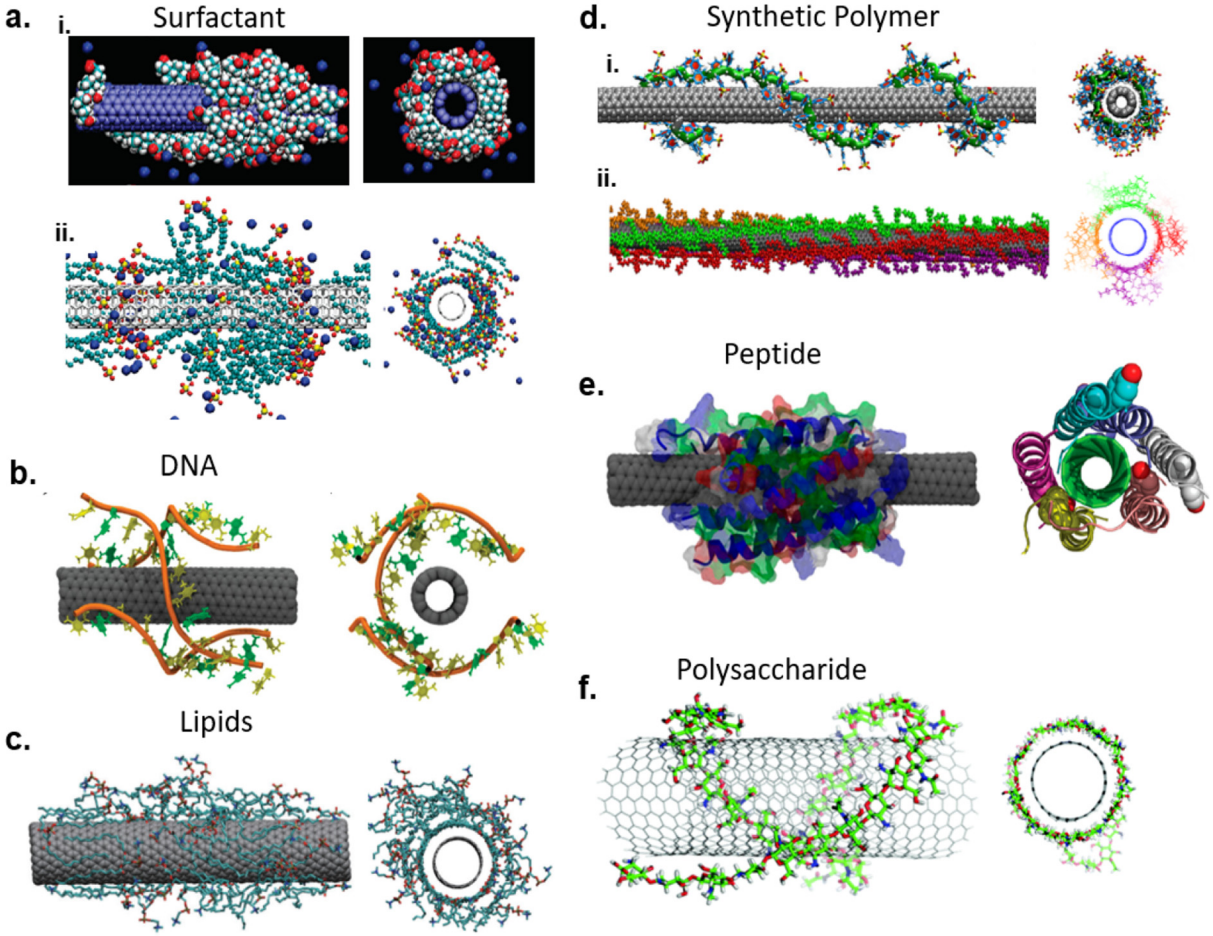

Fig. 2 Non-covalently functionalized SWCNT molecular assemblies with dispersants: (a) surfactant-SWCNT dispersion *via* sodium cholate (i)[169] and sodium dodecyl sulfate (ii);[170] reprinted with permission from ref. 169 and 170. Copyright 2010 American Chemical Society and 2009 American Chemical Society. (b) DNA-SWCNT dispersion;[38] reprinted with permission from ref. 38. Copyright 2012 American Chemical Society. (c) Lipid-SWCNTs dispersion *via* dipalmitoylphosphatidylcholine (DPPC);[34] reprinted with permission from ref. 34. Copyright 2010 Springer Nature. (d) Polymer–SWCNT dispersion *via* poly(styrene-*co*-sodium styrene sulfonate (PS-*co*-PSS, i)[171] and dioctyl substituted polyfluorene (PFO, ii);[172] reprinted with permission from ref. 171 and 172. Copyright 2020 John Wiley and Sons and 2015 American Chemical Society (e) peptide-SWCNT dispersion with HexCoil-Ala;[35] reprinted with permission from ref. 35. Copyright 2013 American Chemical Society. (f) Chitosan wrapped SWCNT.[37]

SWCNT biocompatibility as well as expand their applications as optical probes and carriers for drug delivery or imaging.[39,44–46]

Recently, researchers have introduced sp^3 defect chemistry approach to covalently functionalize SWCNTs while preserving their optical properties and increasing their quantum yield. The sp^3 quantum defects/luminescent defects, also known as organic color centers (OCC), are created *via* covalently bonding aryl or alkyl groups onto sp^2 lattice on SWCNTs.[47,48] A localized two-level electronic state within the nanotube's electronic structure is introduced *via* OCCs allowing for electronic transitions of excitons (Fig. 3a). This enables single-photon emission in the NIR region due to the OCC's localization and trapping of excitons resulting in significant red-shifting from the original E_{11} position, generally referred to E_{11}^{*}.[48,49] Moreover, functional groups, defect densities, and chemical environments can affect PL on defect-induced nanotubes.[48] This phenomenon has opened new opportunities for controlled covalent functionalized SWCNTs for NIR sensing and imaging applications. Kwon *et al.* introduced sp^3 defects on nanotubes through aminoaryl functionalized SWCNTs and utilized these nanotubes in monitoring temperature and pH changes (Fig. 3b).[49] The protonation and deprotonation of the amino group on the SWCNT defect site resulted in PL changes in response to pH changes. Using nanotubes in serum media, the authors demonstrated that this sensor could respond to pH changes as low as 0.2 pH units over the biologically relevant pH range (pH 4.5 to pH 8.5).[49] Furthermore, they discovered a quenching effect in nanotube fluorescence with increase in temperature (15 °C to 85 °C).[49] This study opened new opportunities for biosensing with OCC-SWCNTs.

SWCNTs as optical nanosensors

For a SWCNT-based nanosensor, the dispersant on the nanotube surface acts as a targeting element and nanotube itself

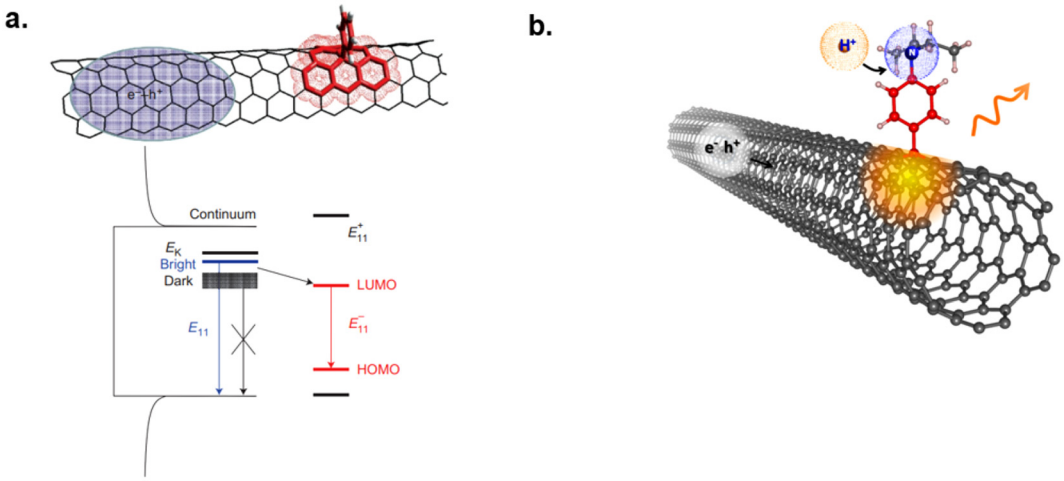

Fig. 3 Organic color center-based SWCNTs sensors. (a) Inducing sp^3 quantum defects onto sidewall of SWCNT *via* covalent attachment of an aryl group.[47] The quantum defect allows for a localized two-level electronic state within the nanotube's electronic structure enabling entrapment and electronic transitions of excitons.[47] Reprinted with permission from ref. 47. Copyright 2013 Springer Nature. (b) OCC-SWCNT for monitoring pH and temperature changes.[49] Reprinted with permission from ref. 49. Copyright 2015 American Chemical Society.

acts as a transducer. Thus, a SWCNT-based optical sensor system comprises three main components: a molecular targeting element, a transducer, and a signal processing unit.[1] The molecular targeting element interacts with the target analyte, the transducer translates the physical or chemical change that takes place upon specific molecular recognition, and the signal processor produces the signal output.[1] For example, the surface functional coatings on SWCNTs including DNA, polymer, lipids, and other small molecules act as the molecular targeting elements to facilitate specific molecular recognition with the target analytes. Nanotubes are very sensitive to their local physicochemical environment. Thus, changes in the surrounding environment including polarity, pH, dielectric, surface charge, *etc*. can induce fluorescence enhancement, quenching, or red/blue emission wavelength shifts as shown in Fig. 4.[2,50] The optical changes are processed by signal processor which produces the fluorescence spectrum for observation of emission changes.

Sensing mechanisms

The exciton travels along the nanotube axis, visiting tens of thousands of carbon atoms during its lifetime.[5,14] Photoluminescence from the nanotubes occurs when the exciton recombines through radiative relaxation. The range that the exciton travels can be affected by factors such as nanotube chirality,[51] functionalization,[15] and defect density.[5] Furthermore, an exciton's travel can be disrupted through changes in the local environment such as increase in dielectric, withdrawing of electrons, or reduction in nanotube's electron density, nonradiative recombination sites may be induced resulting in fluorescence quenching.[5,50] The sensing mechanism of SWCNT optical sensors can be based on the polarity of the solvent, dielectric environment, charge transfer, and redox mechanisms (*vide infra*). Understanding these mechanisms is important as this produces the output needed to enable sensor function *via* changes in fluorescence intensity and/or wavelength.

Fluorescence modulation *via* solvatochromism

One of the mechanisms of fluorescence modulation is *via* solvatochromic shift of the fluorescence, which takes place when a molecule experiences a change in its dipole moment due to external stimuli/factors upon photoexcitation.[52] The solvent molecules which surround the nanotubes reorient to solvate the dipole,[52,53] creating a difference in the solvation energy between the molecule in the excited and ground states and causing a solvatochromic shift.[52] Choi and Strano studied this phenomenon on SWCNTs by considering semiempirical scaling model that describes the spectral shift resulting from the differences in the exciton polarizability of SWCNT in various media. A pristine SWCNT is highly polarizable but has no net dipole moment. A dipolar solvent can induce a dipole moment and the PL shift is proportional to the difference in SWCNT polarizability between the ground and the excited states of E_{22} transitions. The authors reasoned that the difference in the polarizability between the ground and excited states for SWCNT is determined by the polarizability of the exciton.[52] This scaling model was used to explain the observed PL shifts for SWCNTs in various dielectric environments. The model could be used to predict solvatochromic shifts of SWCNTs in various dielectric environments. Silvera-Batista *et al.* and Larsen *et al.* further explored the effect polarity and dielectric constants have on nanotube fluorescence. It was reported that SWCNT quantum yield is strongly dependent on polarity and electrophilicity of a solvent.[53,54] Furthermore, solvatochromic shifts are correlated with the extent of SWCNT solvation.[54] For example, nanotube fluorescence will experience intensity quenching and emission wavelength red shift-

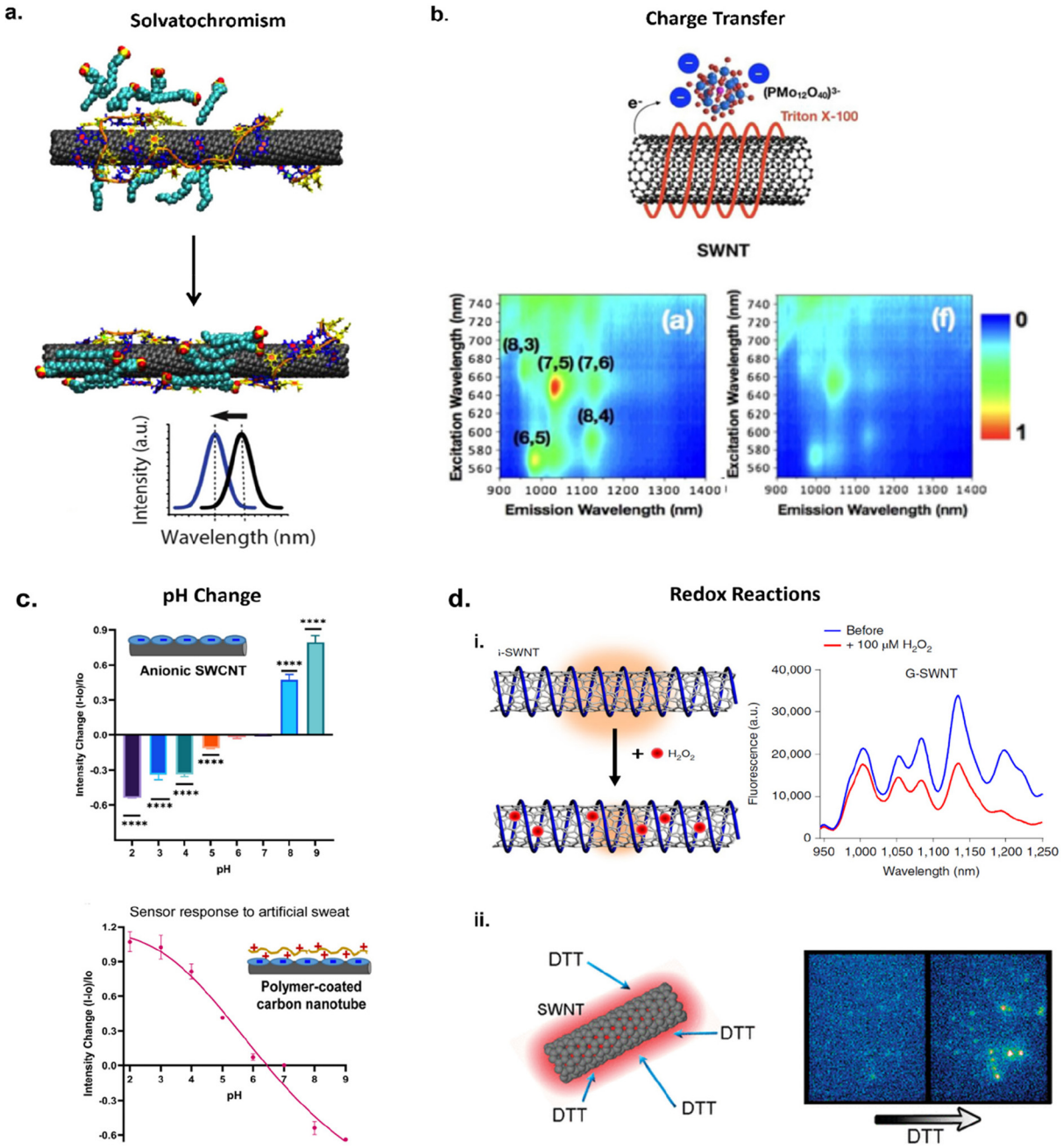

Fig. 4 Examples of optical sensing mechanisms: (a) solvatochromic shifting of SWCNT fluorescence *via* modulation of nanotube surface coverage. Interactions of surfactant SDBS with ssDNA–SWCNTs allow for increased surface coverage inducing blue-shifting in nanotube fluorescence.[173] Reprinted with permission from ref. 173. Copyright 2018 American Chemical Society. (b) Charge transfer between Triton X-100-SWCNT complex and phosphomolybdic acid (PMo_{12}). Anionic dopant PMo_{12} interactions with nonionic SWCNTs allow for electron transfer from the nanotube to PMo_{12} causing a quenching effect in nanotube fluorescence;[58] Reprinted with permission from ref. 58. Copyright 2017 John Wiley and Sons. (c) Modulation of SWCNT fluorescence *via* pH changes in aqueous solution with anionic SWCNTs and artificial sweat with polymer coated SWCNTs;[174] (d) Oxidation (i) and reduction (ii) interactions with SWCNTs. Oxidation occurs *via* adsorption of H_2O_2 onto ssDNA–SWCNTs causing disruption of excitonic travel thereby quenching fluorescence.[62] Reprinted with permission from ref. 62. Copyright 2020 Springer Nature. Reducing agent dithiothreitol (DTT) adsorption onto SWCNT surface passivates hole-doped defects on SWCNT enabling a brightening effect in NIR fluorescence.[59] Reprinted with permission from ref. 59. Copyright 2011 American Chemical Society.

ing in highly polar solvents while fluorescence intensity enhancement and emission wavelength blue shifting occurs in nonpolar solvents.[53,54] The inverse relationship between solvent polarity and SWCNT fluorescence can be attributed to the solvent dielectric. When a SWCNT is in a polar solvent, there is an increase in dielectric screening of the exciton due

to coulombic interaction by the solvent molecules thereby reducing radiative exciton recombination.[53–55] This was found to be true for solvents with increasing dielectric constants.[53,55] Therefore, changes in the microenvironment surrounding the nanotube surface, such as surface water molecules displacement in aqueous-suspensions of SWCNTs, can induce fluorescence modulations. Solvatochromic shifts can also be a result of conformational changes in the polymer that encapsulates a nanotube, or reorganization of small molecules bound to the nanotube surface. These changes in the coverage of the nanotube surface could expose or shield the exciton to the surrounding environment,[52,56] resulting in a shift in emission wavelength as demonstrated in Fig. 4a.

Fluorescence modulation *via* charge transfer

Fluorescence modulation can also occur *via* charge transfer of electrons between the nanotube, dispersant, solvent, and analytes. This can occur *via* an overlapping of nanotube and analyte orbitals where electrons are withdrawn from the π-system of the nanotube surface, creating sites for nonradiative recombination thereby quenching fluorescence.[2,54] The fluorescence modulation through charge transfer include electron transfer from the top of the valence band of SWCNTs to the lowest unoccupied molecular orbital (LUMO) of the analyte,[57] decrease in electron density through electrophilic solvents,[54] and a functionalizing molecule/dispersant acting as the electron withdrawing substituent which shifts SWCNT Fermi levels into the valence band resulting in quenched emission.[25] Hong *et al.* demonstrated charge transfer by doping TritonX-100-SWCNTs complexes with phosphomolybdic acid (PMo_{12}), a common polyoxometalate that can act as an electron acceptor.[58] Due to the difference in Fermi levels between SWCNTs and PMo_{12}, their interactions lead to naturally occurring charge transfer with SWCNTs as electron donors and PMo_{12} as electron acceptors.[58] NIR fluorescence measurements showed quenching of nanotube emissions with the addition of PMo_{12} (Fig. 4b). Control experiments, which included using SWCNTs wrapped with anionic carboxymethyl cellulose sodium salt (Na-CMC) did not exhibit a quenching effect in the presence of PMo_{12}. This was attributed to the difference in types of the two surfactant/polymer–SWCNT complexes tested. Na-CMC was not able to stabilize the donor–acceptor hybrid structure due to the negative charge of the dispersant repelling the negatively charged PMo_{12} [58] whereas nonionic TritonX-100 allowed for stabilization of the donor–acceptor structure leading to efficient charge transfer. Thus, this study demonstrated how charge transfer can be tuned by changing the surface functionalization and its effects on PL.

Fluorescence modulation *via* redox reactions

Fluorescence can be modulated through redox reactions on SWCNTs. For example, it has been reported that reducing agents such as dithiothreitol (DTT) can enhance nanotube fluorescence (Fig. 3dii) by passivating hole-doped defect sites through donation of electrons.[59] This enhancement was reversed by removing the reducing agents, suggesting that fluorescence quenching is due to the defect sites which can be induced by oxidation of the nanotube surface *via* oxygen atoms.[59,60] Fluorescence quenching due to oxidation can occur through electron transfer from the top of the valence band in the carbon nanotube to the oxidizing agent (oxygen atom) reducing nanotube electron density and creating partial positive charge on the surface.[60,61] Thus, the nanotube's electronic structure is perturbed, thereby introducing a defect site and increasing nonradiative recombination pathways. The output results in quenching and a red shifted fluorescence spectrum.[61] Lew *et al.* demonstrated this sensing mechanism by developing a nanosensor for monitoring wound-induced hydrogen peroxide (H_2O_2) signaling in plants.[62] SWCNTs were functionalized with $ss(GT)_{15}$ (G-SWCNTs) and exposed to 100 μM H_2O_2 *in vitro*. The nanotube's fluorescence quenched in the presence of H_2O_2, which was attributed to electron transfer from SWCNTs to H_2O_2 because of adsorption onto the nanotube surface (Fig. 3di). Furthermore, the nanotube's response to H_2O_2 was reversible through the addition of catalase which converts H_2O_2 into H_2O and O_2. The nanotube signal recovered to its original brightness within a few minutes after catalase addition.[62]

Advances in optical nanosensor development

SWCNTs-based sensors have been developed for the detection and imaging of various molecules including neurotransmitters,[63] proteins,[64,65] mRNAs,[66,67] COVID-19 virus,[68] protein tags and hydrogen peroxide,[69,70] lipids,[71] and chemotherapy drugs *etc*. (Fig. 5a–f). These optical sensors were employed for studies that involve sensing/detection in solution, *in vitro*, *in vivo* (small animals) and in plants.[67,72,73]

Detection of steroid hormones

Steroid hormones play an important role in many physiological processes including growth, development, energy metabolism, and reproduction.[74] Imbalance of hormones can lead to health issues such as diabetes, cancer, infertility, and dysregulation of neurocognitive functions.[75–77] Thus, monitoring steroid hormones could help facilitate early disease diagnosis and treatment. Studies conducted by Zhang *et al.* and Lee *et al.* show that nanotube-based sensors could be utilized for hormone detection. Zhang *et al.* reported molecular recognition of estradiol, a sex hormone that is responsible for maintaining the female reproductive system, bone maintenance, nitric oxide production, and brain functions,[78,79] with SWCNTs functionalized with rhodamine isothiocyanate-difunctionalized poly(ethylene glycol) (RITC-PEG-RITC).[80] This was done by screening several synthetic heteropolymers in which RITC-PEG-RITC-SWCNTs exhibited a quenching in nanotube fluorescence specific to estradiol. This was hypothesized to be due to desorption of the RITC groups from the nanotube surface during interactions with estradiol, causing decreased surface coverage and ultimately quenched nanotube

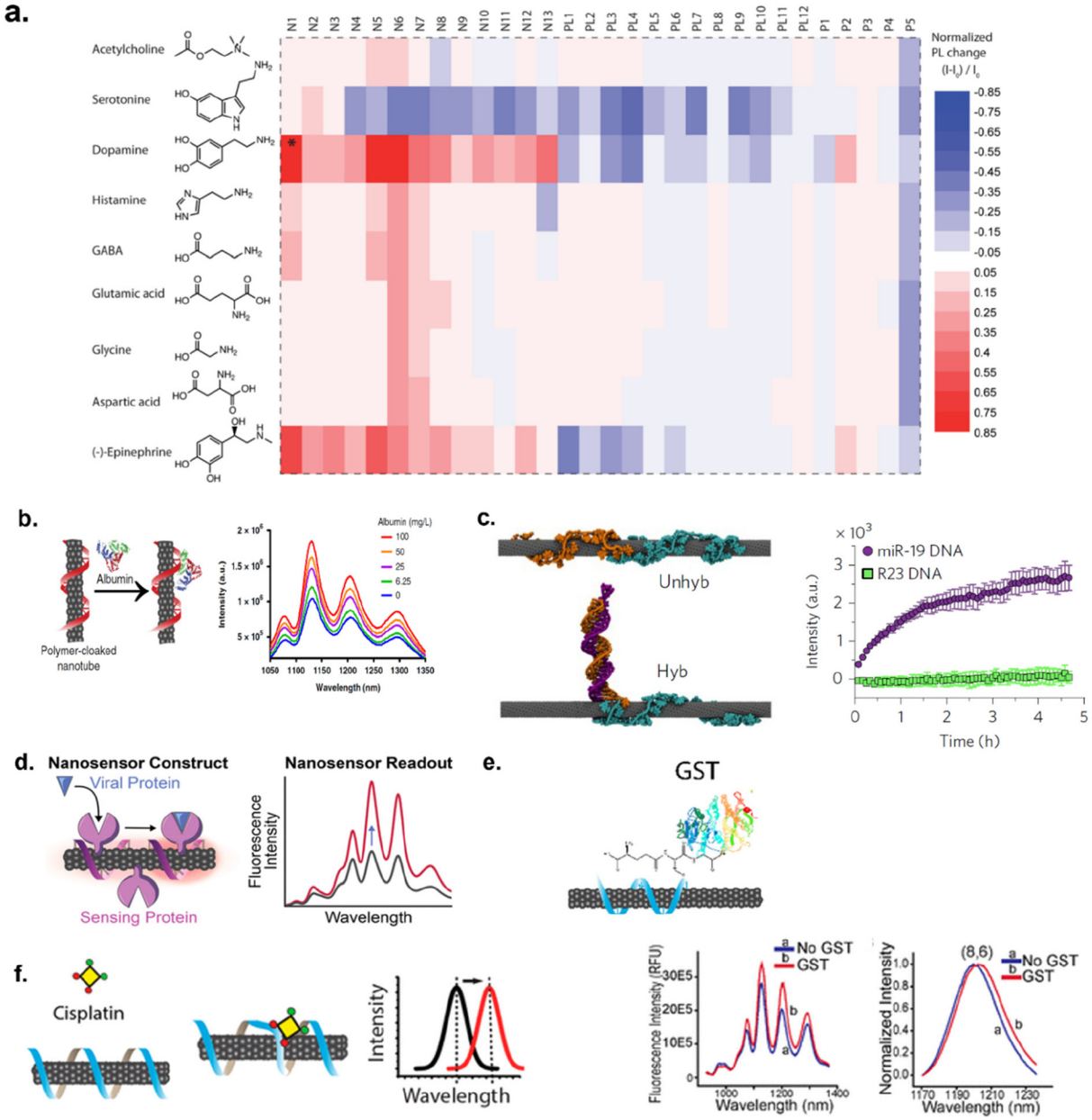

Fig. 5 Examples of target analytes detected by SWCNTs. (a) Heat map of SWCNTs optical response to neurotransmitters *via* screening a library of sensors against nine different neurotransmitters.[63] Reprinted with permission from ref. 63. Copyright 2014 American Chemical Society. (b) Detection of protein, albumin, *via* polymer-cloaked SWCNTs.[64] Reprinted with permission from ref. 64. Copyright 2019 Springer Nature. (c) MD simulation snapshot of RNA-DNA hybridization events for detection of miRNA.[67] Reprinted with permission from ref. 67. Copyright 2017 Springer Nature. (d) Detection of COVID-19 virus spike protein.[68] Reprinted with permission from ref. 68. Copyright 2021 American Chemical Society. (e) Adsorption of protein tag, glutathione-*S*-transferase (GST), to ssDNA–SWCNTs.[69] Reprinted with permission from ref. 69. Copyright 2020 American Chemical Society. (f) DNA-SWCNT response to chemotherapeutic drug, cisplatin.[175] Reprinted with permission from ref. 175. Copyright 2017 American Chemical Society.

emissions.[80] Furthermore, it was concluded that the conformation of the polymer on the nanotube surface played a significant role in specific molecular recognition. Thus, small changes in polymer composition or nanotube chirality could result in a new arrangement of the polymer on the nanotube surface and yield different binding sites for molecular recognition to occur. Lee *et al.* used similar methods to monitor steroid hormones *in vivo*. In this study, a library of amphiphilic polymers containing acrylic acid (hydrophilic unit), styrene (hydrophobic unit), and acrylated cortisol were synthesized *via* RAFT polymerization for encapsulation of SWCNTs for sensor development and screening.[81] Acrylated cortisol was used as a template for hormones of similar sizes and shapes to adsorb onto the nanotube surface. The hypothesis was that when the

sensor is exposed to free hormones in bodily fluids, the acrylated cortisol would desorb from the nanotube surface allowing for a binding site to become available. The adsorption of free hormones would cause the dispersant polymer to change its conformation on the nanotube surface thereby triggering a change in SWCNT fluorescence. The sensor screening against 11 steroid hormones revealed an affinity towards progesterone, a female sex hormone that plays an important role in menstruation and pregnancy. Additionally, the optimal nanosensor for progesterone from the screening assay was then incorporated into hydrogels. Furthermore, reversibility of the sensor-in the hydrogel complex was established by exposing to alternating cycles of 0–100 μM of progesterone in buffer solution. The sensor's response recovered to its original baseline and consistently responded with each cycle for hormone exposure. The sensor, embedded in the hydrogel matrix, also responded to progesterone in mouse serum. Once the sensor response was established within the hydrogel matrix, the sensor embedded in the hydrogel was implanted into mouse models for *in vivo* measurements. Two sets of sensor-hydrogels were inserted into separate 6–8 kDa dialysis bags (one incubated with 100 μM of progesterone and the other in buffer as the control) to prevent interference from non-specific molecules and these were implanted subcutaneously in mice. There was an immediate response from the treated sensor after implantation with a decreased fluorescence intensity. The change in the optical response was considered a dilution effect as interstitial fluid diffused through the dialysis bags and diluted the amount of progesterone present. Additionally, tissue samples were examined for inflammation 28 days after the SWCNT-hydrogels were implanted in which resolution of the acute inflammatory response and encapsulation in an epithelioid cap were observed, demonstrating biocompatibility. This study demonstrated the development and application of SWCNT-based progesterone sensor for *in vitro* and *in vivo* studies.

Detection of cancer biomarkers

Carbon nanotube-based sensors have been investigated for cancer diagnosis. This has been done *via* taking advantages of specific molecular interaction between an antibody and cancer biomarkers. A more common approach to develop SWCNT nanosensor for cancer detection includes conjugating antibodies specific to cancer biomarkers onto the nanotube surface to facilitate tailored molecular interactions between the nanosensor and target biomarker. For example, Welsher *et al.* conjugated Rituxan, an antibody that recognizes B-cell lymphoma cells, onto SWCNTs functionalized with polyethylene glycol (PEG) for detection of B-cell lymphoma. Additionally, Herceptin, an antibody that recognizes breast cancer cells, was conjugated onto PEG-SWCNTs for the detection of breast cancer cells.[82] The SWCNT–antibody complexes were incubated with the B-cell lymphoma and breast cancer cell lines separately and imaged *via* NIR fluorescence imaging *in vitro*. Each antibody–SWCNT complex exhibited an increased fluorescence response to their respective cell lines (Fig. 6a). This study demonstrated how SWCNT-based sensors can be used to detect cancer cells. Williams *et al.* reported the detection of prostate cancer *in vitro*[83] and ovarian cancers[84]

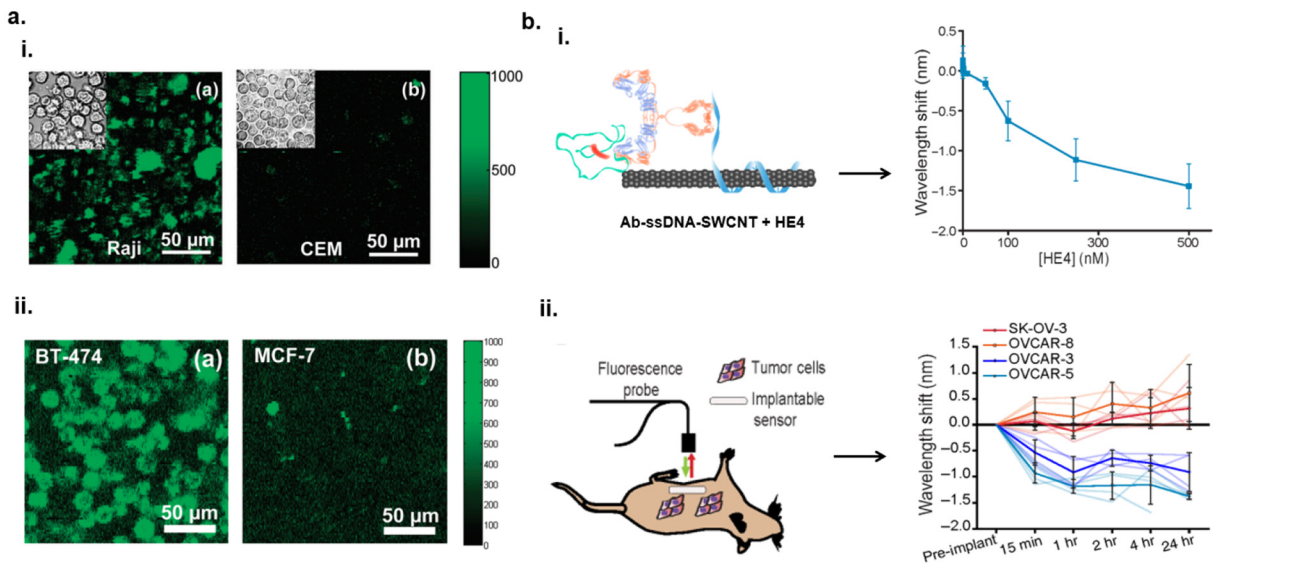

Fig. 6 Detection of cancer biomarkers *in vitro* and *in vivo*. (a) NIR fluorescence images of B-cell lymphoma cells (Raji cells) and control T-cell lymphoma (CEM) cells in the presence of Rituxan-SWCNTs (i). NIR fluorescence images of breast cancer cells (BT-474) and control MCF-7 cells in the presence of Herceptin-SWCNTs (ii).[82] Reprinted with permission from ref. 82. Copyright 2008 American Chemical Society. (b) Ab-ssDNA–SWCNT optical response to the presence of HE4, biomarker for ovarian cancer, *via* blue-shift in nanotube emissions with increase in HE4 concentration (i). Schematic of *in vivo* measurements *via* NIR optical probe of Ab-ssDNA–SWCNTs in mouse model with various tumor cell lines expressing HE4 (ii). SK-OV-3 and OVCAR-8 were HE4 negative exhibiting minimal to slight red-shifting of nanotube fluorescence. OVCAR-3 and OVCAR-5 were HE4 positive and demonstrated blue-shifting.[84]

in vivo. To enable the detection of prostate cancer, antibody conjugated SWCNTs were employed. An antibody for specific binding of urokinase plasminogen activator (uPA), a biomarker protein for prostate cancer, was conjugated *via* carbodiimide crosslinking chemistry onto SWCNTs functionalized with amine modified single-stranded DNA (ssDNA). The sensor exhibited sensitivity to uPA with a limit of detection at 25 nM in fetal bovine serum (FBS)-enriched media.[83] Furthermore, the nanotube's response in human whole blood samples exhibited similar red-shifting in the fluorescence as was observed in FBS media. The red-shifting was attributed to an accumulation of electrostatic charge density close to the nanotube surface, causing an increase in the dielectric environment. This study demonstrated the advancement of nanotube-based sensors for cancer biomarker detection in biofluids.

Williams *et al.* reported optical nanosensors for ovarian cancer detection in patient biofluids and *in vivo* using small animal models.[84] Using the same methodology as mentioned, an antibody specific towards human epididymis protein 4 (HE4), was conjugated onto ssDNA–SWCNTs to develop Ab-ssDNA–SWCNT nanosensor. This sensor could detect HE4, an FDA approved biomarker for ovarian cancer diagnosis, with an LOD between 1 and 2.5 nM in patient biofluids.[84] For *in vivo* studies, the sensor was loaded into a semi-permeable membrane tube and the sensor construct was implanted into mice exhibiting ovarian cancer tumors. A fiber optic probe connected to a NIR spectrometer was used for noninvasive measurements of the nanotubes' optical responses from within the mouse. The sensor exhibited a blue-shift in wavelength to HE4 which was consistent with the results observed in patient biofluids (Fig. 6b). The mechanism behind the spectral blue-shift was hypothesized to be due to the interactions between the antibody and the protein biomarker thereby displacing water molecules from the nanotube surface. This type of nanosensor constructs show promise for use in clinical settings in cancer diagnosis and monitoring therapies.

Detection of pathogens (bacteria and viruses)

Early detection of pathogens could aid in early diagnosis and treatment of infectious diseases to combat a rise in antibiotic-resistant infections.[85] Nißler *et al.* designed a library of non-covalently functionalized DNA-SWCNT-assemblies that could aid in the detection of metabolites including lipopolysaccharides, siderophores, DNases, and proteases released from pathogens and virulence factors.[86] These SWCNT-based sensors were further integrated into polyethylene glycol-based hydrogels and the nanosensors were remotely imaged with NIR stand-off detection (Fig. 7a). The sensor array was exposed to six clinically relevant bacteria which cause post-surgery infections in artificial joint implants. The optical responses from the sensor arrays with distinct DNAs on the nanotube surface provided fingerprinting of *E. coli*, *S. aureus*, *S. epidermidis*, and *P. aeruginosa* (Fig. 7a). Furthermore, differentiation between

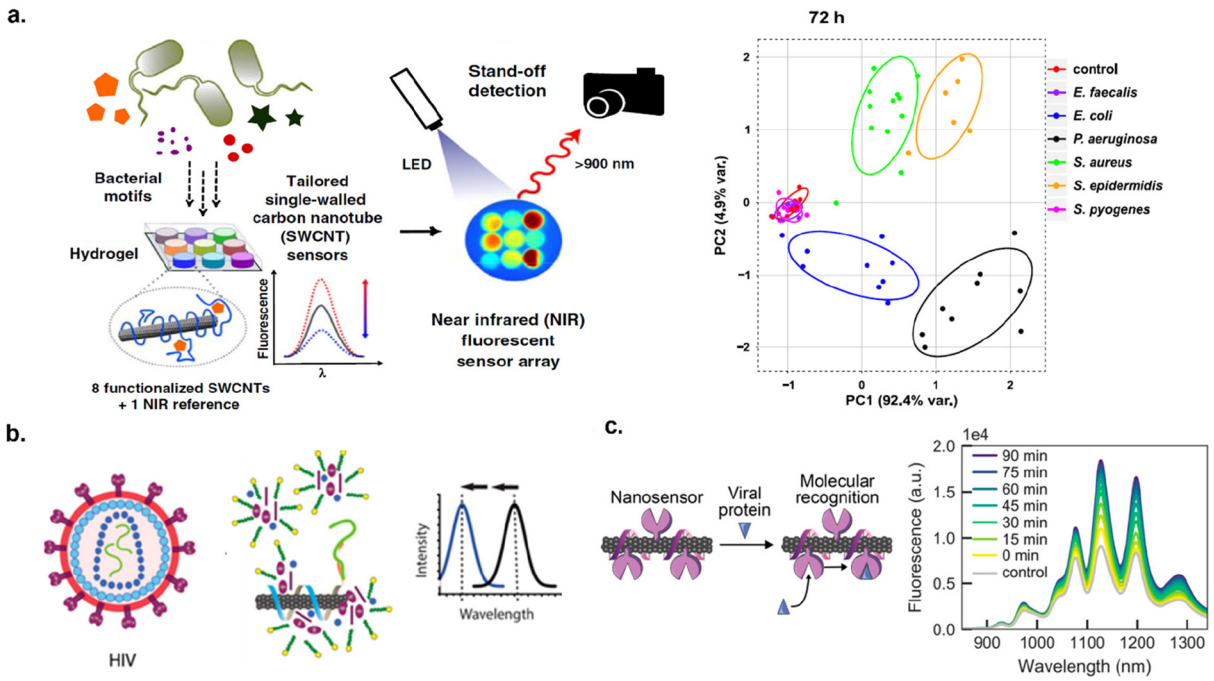

Fig. 7 Detection of pathogens. (a) Schematic of SWCNT-based sensors incorporated into hydrogel sensor array for the optical detection of bacteria. NIR measurements were conducted remotely *via* stand-off detection. Optical responses yielded differentiation of bacterial species.[86] Reprinted with permission from ref. 86. Copyright 2020 Springer Nature. (b) Schematic of SWCNT-based sensor for detection of human immunodeficiency virus (HIV).[66] Reprinted with permission from ref. 66. Copyright 2019 American Chemical Society. (c) Detection of spike (S) protein from SARS-CoV-2 virus *via* DNA functionalized SWCNTs with angiotensin-converting enzyme 2 (ACE2) receptor. The sensor detected S protein through increased NIR emissions.[68] Reprinted with permission from ref. 68. Copyright 2021 American Chemical Society.

species of bacteria was established. This could aid in timely diagnosis of bacterial infections.

Shumeiko *et al.* developed an optical nose consisting of an array of peptide-encapsulated SWCNTs on a paper substrate for detection of bacteria.[87] Peptides-functionalized nanotubes were used to develop a wide array of sensors with varying combinations of natural and unnatural amino acids in peptides. Using sixteen different peptides containing tyrosine in different proportions and positions with aspartic acid, glutamic acid, lysine, and Fmoc-lysine, the authors determined that peptides containing tyrosine, lysine, and/or Fmoc-lysine with longer chains dispersed nanotubes at higher concentrations with enhanced photoluminescence (PL) signals. The sensors drop-casted onto a paper substrate were exposed to volatiles/smell from *E. coli* and *K. pneumoniae* within bacterial culture. The sensors exhibited a significant PL increase ranging from 8–22% to both bacterial strains within 60 seconds of exposure to volatiles. Solvatochromic shifting caused by conformational changes in the encapsulating peptide could have contributed to the PL increase. Additionally, repeated exposures to bacterial smells were measured to characterize the sensor's functionality and reusability. After each exposure cycle, the sensors were allowed to recover to baseline with clear airflow. It was observed that the recovery signals over 300 seconds from the sensors allowed for classification between the two bacterial species tested. Therefore, this method could be advantageous for conducting rapid diagnostics for early detection of bacterial infections with optical sensing of volatile organics from pathogens.

SWCNT-based sensors have also been explored for detection of viruses. Harvey *et al.* reported a SWCNT nanosensor for the detection of human immunodeficiency virus (HIV) in serum (Fig. 7b).[66] The sensor was composed of SWCNTs noncovalently functionalized with GT_{15}miR19 a sequence complementary to target miR19 oligonucleotide.[66] The sensor was exposed to intact HIV particles, SDS, a common surfactant used in protein denaturation, and target oligonucleotide to bind to GT15miR19 SWCNTs, nanotubes showed changes in optical responses. The proposed mechanism describes that SDS denatured the HIV envelope and released viral protein, that could be adsorbed onto the nanotube surface to elicit the changes. The nanotube's response was significantly higher in the presence of complimentary sequence when compared to addition of oligonucleotide with a non-complimentary sequence.[66] This study could be expanded to detection of other viruses in serum.

Pinals *et al.* reported SWCNT-based sensors for the detection of COVID-19 virus. SWCNTs were functionalized with DNA and incubated with angiotensin-converting enzyme 2 (ACE2) receptor to passivate the protein onto the nanotube surface. Virus detection was facilitated by binding the spike (S) protein to the sensor.[68] The nanosensor exhibited enhanced fluorescence within seconds upon exposure to S protein, where intensity enhancement occurred overtime and reached 99.6% enhancement after 90 minutes (Fig. 7c).[68] Control experiments consisted of exposing the nanosensor to buffer solution without target protein. In the control experiment, the nanotube fluorescence increased less than 25% after 90 minutes. The authors then tested the sensor response in serum and biofluids such as saliva and nasal fluid. While the sensor retained its response in serum, a diminished effect was observed in saliva and nasal fluid.[68] This was attributed to non-specific protein adsorption onto the sensor surface, causing reduced recognition of the S protein. To mitigate these biofouling effects,[88] passivation techniques were used involving phosphatidylethanolamine phospholipid with a PEG chain (PE-PEG) which only exhibited partial improvement.[68] Although this sensor had a lower sensitivity compared to current COVID-19 detection methods,[68] the response was faster compared to polymerase chain reaction (PCR)-based and non-PCR-based techniques in sample processing time. Further antifouling strategies could be investigated to develop nanosensors for a rapid and sensitive point-of-care diagnosis.

Detection of disease biomarker proteins

Proteins play an important role in many physiological processes including pH and fluid balance, regulation of gene expression, driving metabolic reactions, and immune system support.[89] Proteins can also serve as biomarkers for diseases. Thus, detection of proteins could aid in disease diagnosis, facilitate therapies, and help understand biological processes to gain insights to metabolic and signaling pathways.[90] SWCNT-based sensors have been engineered for protein recognition.[91] Landry *et al.* developed a sensor for label free detection of individual proteins secreted from various cell lines including *E. coli* (bacteria) and *P. pastoris* (yeast).[92] The sensor consisted of a noncovalently attached aptamer anchor polynucleotide onto $(AT)_{11}$–SWCNTs. A 53% decrease in nanotube fluorescence upon exposure to 3 μM of RAP1, a protein vital for T-cell signaling pathways, was observed. The SWCNTs' sensitivity to protein secretion from those microorganisms was tested *via* immobilizing the sensors in a microfluidic chamber and incubating sensors in the presence of induced RAP1 secretion from *E. coli* (Fig. 8a). A turn-on response from SWCNTs was observed within 0.5 seconds of exposure to RAP1 in cell lysates. Furthermore, the nanosensor responded to HIV1 integrase with an increased fluorescence intensity up to 48%. The fluorescence change was attributed to changes in the dielectric environment during molecular recognition. They further extended the sensor model to detect HIV1 integrase from human embryonic kidney (HEK293) cells and yeast cells – eukaryotic protein expression hosts. Thus, this study provided a new pathway for studying eukaryotic protein secretion at the single-cell level.

Corona phase molecular recognition (CoPhMoRe) techniques have also been used to engineer SWCNT-based optical probes for protein detection. This technique refers to the use of a compositionally designed heteropolymer that adsorbs onto a carbon nanotube surface for molecular recognition of a target analyte. Analyte binding triggers either a SWCNT near-infrared (NIR) fluorescence intensity change or wavelength shift.[80] Bisker *et al.* employed CoPhMoRe technique for the

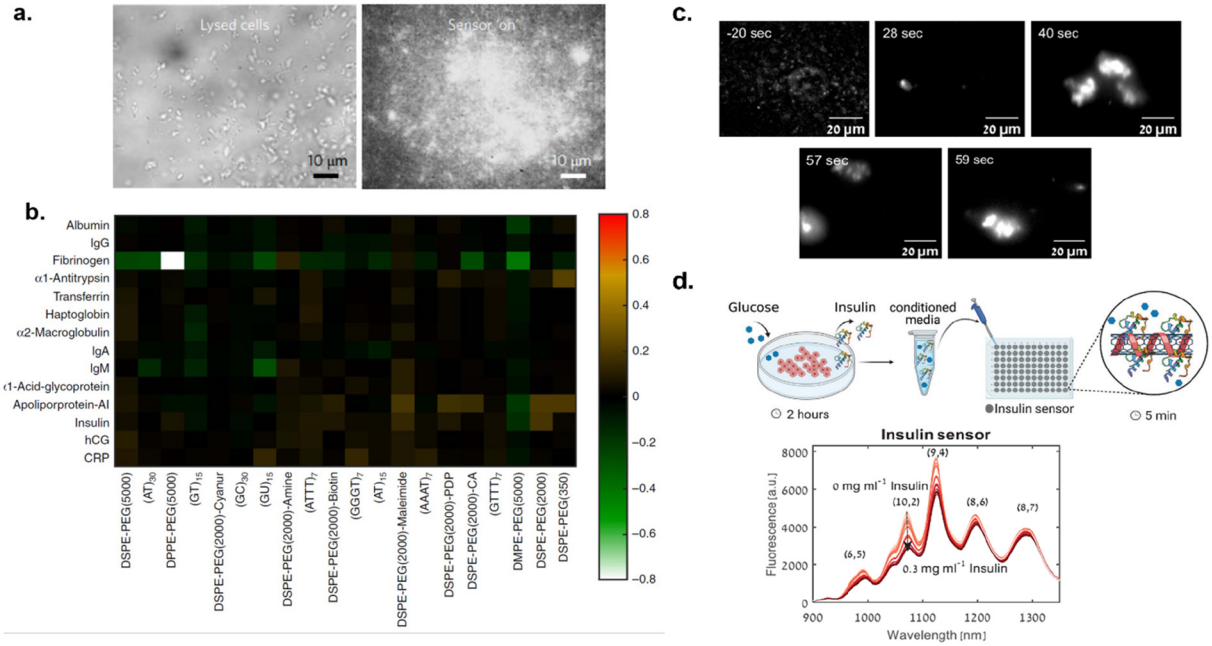

Fig. 8 SWCNT-based detection of disease biomarker proteins. (a) Brightfield and NIR fluorescence images of $(AT)_{11}$–SWCNTs response to RAP1 in *E. coli* cell lysates.[92] Reprinted with permission from ref. 92. Copyright 2017 Springer Nature. (b) Library screening of phospholipid-PEG functionalized and DNA functionalized SWCNTs against fourteen blood proteins *via* corona phase molecular recognition. Specificity towards fibrinogen (indicated with a white box) was determined.[93] (c) NIR fluorescence images of phospholipid-PEG-SWCNTs during clotting process over time. Thrombin, which catalyzes conversion of fibrinogen into fibrin, was added at 0 seconds.[94] (d) Schematic of SWCNT-based insulin sensing from pancreatic cells. Emission spectra of SWCNTs in presence of increasing concentration of insulin.[98] Reprinted with permission from ref. 98. Copyright 2021 John Wiley and Sons.

detection of fibrinogen,[93] a protein that is associated with blood coagulation and platelet aggregation. SWCNTs were non-covalently functionalized with phospholipid-PEG polymer derivatives and these SWCNT complexes were screened against fourteen blood proteins.

The screening revealed that functionalized SWCNTs show specificity towards fibrinogen, which was evident from a greater than 80% decrease in nanotube fluorescence (Fig. 8b).

It was hypothesized that the arrangement of the polymer on the nanotube surface and conformation of fibrinogen facilitated the molecular recognition. This was confirmed with atomic force microscopy (AFM) which revealed the fibrinogen in alignment with the SWCNT axis following adsorption and quartz crystal microbalance with dissipation. The sensor's recognition of fibrinogen was retained in serum environments. Gerstman *et al.* expanded this study to monitor the blood coagulation process in real-time.[94] Using the phospholipid-PEG polymer functionalized SWCNTs, formation of fibrin from fibrinogen during blood clots was studied. Functionalized SWCNTs were incubated with fibrinogen to form SWCNT–fibrinogen complex. Then, thrombin was added to the SWCNT–fibrinogen complex to catalyze the conversion of fibrinogen to fibrin thereby inducing clot formation. The presence of SWCNTs did not seem to hinder the blood clot formation. Furthermore, clot formation process was monitored with NIR imaging of SWCNTs in real-time (Fig. 8c). Thus, these findings could be used to improve diagnostics and therapies for blood clotting disorders. Jin *et al.* also utilized CoPhMoRe methodology for detection of interleukin-6 (IL-6) family of cytokines[95] using SWCNT sensors. IL-6, a cytokine, plays an important role in infection processes, neural functions, and healing processes.[96,97] Thus, monitoring these molecules could provide insight on their relationship to disease processes. Jin *et al.* reported that polymer constructs of amphiphilic polymers consisting of styrene-based copolymers with acrylic acid, styrene sulfonate, and/or diols substituents adsorbed onto SWCNTs responded to IL-6 in solution.[95] A high-throughput screening revealed that among 41 polymer–SWCNT constructs tested, only two polymer–SWCNT constructs showed a dose-dependent response to IL-6. The CoPhMoRe methodology was further employed to develop SWCNT-based sensors for monitoring insulin secretion from pancreatic β-cells.[98] Insulin, a peptide hormone responsible for maintaining blood glucose levels, is secreted from pancreatic β-cells in response to increased blood glucose levels.[99] When secretion of insulin is impaired or defective, diabetes can develop.[100] Understanding pancreatic β-cell mechanisms could provide important insights for diabetes diagnostics and therapies. Bisker *et al.* reported that PEGylated lipid polymer functionalized SWCNTs could recognize insulin in serum.[101] Ehrlich *et al.* further advanced this study by using nanosensors to monitor insulin secretion from pancreatic β-cells upon introduction of glucose (Fig. 8d). Ehrlich *et al.* used natural (insulin aptamer) and synthetic (polyethylene glycol conju-

gated lipid) molecular recognition strategies for nanotube functionalization and insulin detection.[98] It was observed that both the natural and synthetic polymer-SWCNT complexes recognized insulin and showed a decrease in fluorescence intensity by 29% and 16% respectively within 5 minutes of incubation in conditioned media. Furthermore, the LOD was 0.13 μg mL^{-1} which was determined sufficient for measuring insulin from pancreatic β-cells following glucose stimulation.[98] Although both SWCNT complexes responded to the presence of insulin, the synthetic lipid/polymer could be advantageous over natural aptamers for chemical and thermal stability. Thus, nanosensors could be instrumental in advancing diabetes research for improved therapies.

Budhathoki-Uprety *et al.* developed polymer encapsulated nanotube-based sensors for biomarker protein detection. In this study, a nanosensor was developed for the detection of albumin in the urine under microalbuminuria, condition associated with diabetes, cardiovascular diseases, and cancer.[64] Current clinical detection methods for microalbuminuria include immunoturbidimetry (antibody-based) assays, which require specific handling and storage conditions including refrigeration to mitigate reagent degradation.[64] Thus, there is a need for versatile, robust, sensitive, and scalable detection methods. The polymer used to encapsulate the nanotube was designed for mimicking albumin-binding with fatty acids *via* integration of carboxylic acid functional groups in the polymer.[64] Upon exposure to increasing concentrations of albumin, a blue shift in emission wavelength and fluorescence enhancement was observed (Fig. 5b).[64] The PL enhancement and emission wavelength blue-shifting of the nanotubes were attributed to solvatochromic mechanism. Functionalized nanotubes with carboxylic acids could interact with fatty-acid binding sites on albumin creating a more hydrophobic environment around the nanotube surface and displacing water molecules from the nanotube surface. The selectivity and sensitivity in detection were tested by the addition of non-specific proteins to the sensor, which did not yield as strong of a response as with albumin.[64] Furthermore, the sensor retained its sensitivity in patient's urine samples and the functionality was preserved in sensor embedded acrylic paint material.[64] By incorporating the sensor into a solid-state form, a portable and wearable sensor for the development of wearable devices in medical applications could be possible. Thus, a carbon nanotube-based optical sensor could provide ease of production, handling, and storage of sensor material as opposed to detection methods that require antibodies.[64]

Detection of MicroRNAs

MicroRNAs (miRNAs) are small, single-stranded, non-coding RNA molecules that play important roles in regulating gene expression and cellular functions.[102] Dysregulation of miRNAs have been linked to cancer, viral infections, cardiovascular disease, neurological disorders, muscular disorders, *etc.*[102] Thus, these molecules could be used as biomarkers for disease diagnosis. Harvey *et al.* explored a SWCNT-based sensor for the detection of miRNAs *in vitro* and *in vivo* by harnessing RNA-DNA hybridization events.[67] In this study, SWCNTs were functionalized with a DNA sequence that would impart colloidal stability as well as consist of a complementary sequence for hybridization interactions with target miRNA, miR19 for its role in oncogenesis.[67] Upon incubating the sensor with the target miRNAs in urine and serum samples, SWCNTs exhibited a blue shift in wavelength and increased intensity of nanotube fluorescence specific to miR19. The mechanism of detection was described as a result of competitive displacement of electrostatic charge and water molecules from the nanotube surface upon the hybridization event, thereby causing a solvatochromic shift. Reversibility was also determined *via* toehold-mediated strand displacement by introducing toehold, a single-strand overhang on duplexed DNA, to facilitate hybridization with a complementary strand. Once the removing strand was introduced, nanotube fluorescence recovered back to its initial state. Furthermore, *in vivo* functionality was established by implanting the sensor into the peritoneal cavity in mice models. The sensor response was measured noninvasively *via* a fibre-optic probe-based system to evaluate the sensor's response to increasing concentrations of miRNA (Fig. 9a). The sensor detected miRNA up to 100 pM *in vivo* (Fig. 9b), which is within the physiologically relevant range.[67] Thus, SWCNT-based optical probes can be engineered for miRNA detection *in vitro* and *in vivo* for diagnostic applications.

Hendler-Neumark *et al.* engineered sensors to detect miRNAs associated with acute myocardial infarction.[103] Five sensors were developed by functionalizing SWCNTs with DNA sequences that were complementary to the target miRNAs. Upon incubating the sensors with 10 μM of miRNA in buffer, three out of five sensors responded with increases in nanotube fluorescence ranging from 22–53%.[103] The fluorescence modulation was attributed to the hybridization of DNA and RNA with their complementary sequences, causing conformational changes of the DNA on the nanotube surface, which could result in solvatochromic changes on nanotubes. Among those three sensors, only one sensor retained its sensing ability in serum environment. The sensor responded to 10 μM of miRNA with a 125% fluorescence increase. The LOD ranged from 9–81 nM over the nanotube chiralities examined. Additionally, the sensitivity and specificity were tested by exposing the sensor to other mutated and random miRNAs. This resulted in low response from mutated sequences and high specificity towards the target miRNA in the presence of random sequences in serum (Fig. 9c).

Sensing lipids accumulation

Lipid disorders have been associated with neurodegenerative disorders, cancer, artherosclerosis, liver disease, and lysosomal storage disorders.[104–107] Heller Lab developed DNA-functionalized optical reporters for measuring lipid accumulation in cells and *in vivo* and studied a long-term biocompatibility of those sensors in mouse model.[71,108–110] Jena and Roxbury *et al.* developed a sensor that allows detection of lipid flux in the endolysosomal lumen of live cells.[71] By functionalizing

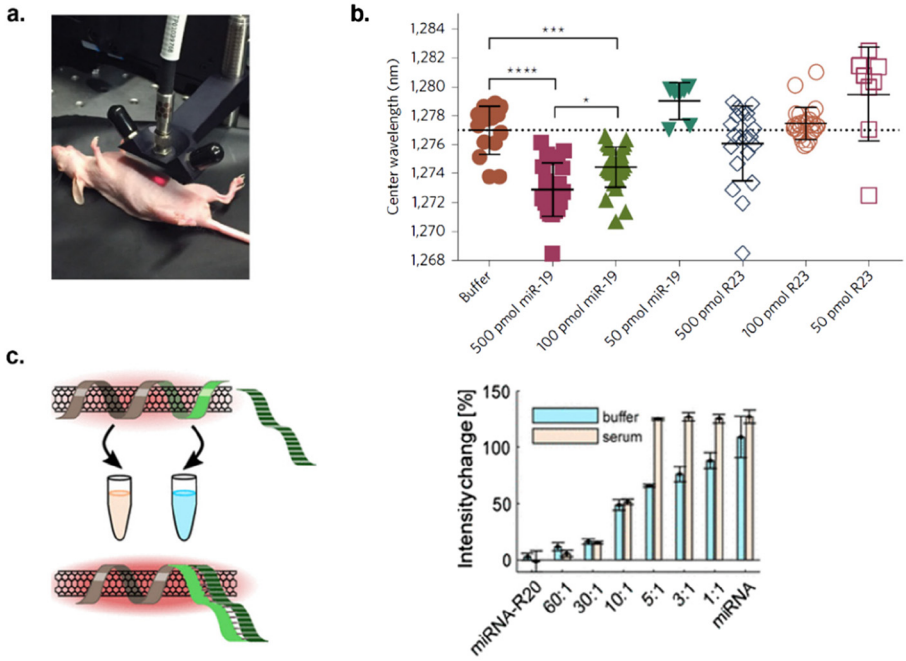

Fig. 9 Detection of microRNA *in vitro* and *in vivo*. (a) Image of NIR probe for measuring sensor response in mouse model. (b) NIR response of SWCNTs to decreasing miR-19 DNA concentration compared to control oligonucleotide sequence.[67] Reprinted with permission from ref. 67. Copyright 2017 Springer Nature. (c) microRNA detection in buffer and serum (left – scheme and right – results). SWCNTs had a specific response to target microRNA in the presence of random RNA sequences in serum.[103]

(8,6) SWCNTs with ss$(GT)_6$ DNA sequence, the authors showed that the sensor responds to lipids. The sensor responded to lipid accumulation within the endolysosomal lumen of live cells *via* wavelength shift in nanotube fluorescence (Fig. 10a and b). The mechanism was illustrated with MD simulations which showed ~19% decrease in the density of water molecules around the nanotube surface upon adsorption of cholesterol and sphingomyelin, lipid molecules present in the endolysosomal lumen and cell membrane.[71] The quantitative detection of lipids within live cells was performed *via* NIR hyperspectral microscopy.[71] The sensors responded to lipid accumulation in cells with lysosomal storage disorders from a patient with Niemann-pick type C disease, a disease that causes abnormal processing of lipids within the body. The results from single-cell kinetics revealed varying lipid accumulation rates among different cells.[71] The sensor localized within the endolysosomal lumen of live cells *via* endocytotic pathways without hindering organelle morphology, structural integrity, or function. This study demonstrated the NIR measurements of lipid flux within live cells which could be used for investigating disease pathways. Galassi *et al.* advanced this study and reported measuring lipid accumulation *in vivo*[109] (Fig. 10c). Using ss$CTTC_3TTC$ – (9,4) SWCNTs, the sensors were intravenously injected into mice models exhibiting Niemann-pick type C disease, atherosclerosis, and non-alcoholic fatty liver disease (NAFLD), all models associated with lipid accumulation disorders. The sensor in each mouse model exhibited a blue shift in wavelength of nanotube fluorescence and allowed for monitoring of lipid accumulation ranging from minutes up to 6 weeks after injection. This indicates that SWCNT-based sensors could be used in monitoring lipid flux *in vivo* which could help in understanding disease biology and aid in the drug discovery and development processes.

Recently, Antman-Passig *et al.* further developed SWCNT-based lipid reporters by monitoring lipid accumulation intracranially.[110] ss$CTTC_3TTC$ – (9,4) SWCNTs were directly injected into mice cerebellum for monitoring of sphingomyelin accumulation (Fig. 10d). This lipid has been associated with Niemann-Pick type A (NPA) disease known to cause rapid neurodegeneration and fatality in infants.[110] NIR fluorescence measurements showed a blue-shift in emission spectra from the nanotubes when compared to the control model, indicating a higher lipid content in NPA presenting mouse models. They also investigated the fate of the sensors in brain tissue *via* NIR hyperspectral microscopy. It was observed that the nanotubes did not cause significant cell damage and the sensors remained near the injection site. This study demonstrated that nanotube optical sensors could be used to monitor lipid accumulation in brain tissue providing a pathway for utilizing optical nanosensors for studying neurodegenerative diseases.

Detection of hydrogen peroxide in biological processes

Hydrogen peroxide (H_2O_2), a byproduct of cellular metabolism, is a reactive oxygen species (ROS) which plays a crucial role in cell signaling.[111] Thus, monitoring H_2O_2 can provide better understanding of cell signaling pathways. Previous studies showed that the introduction of H_2O_2 to SWCNTs quenches

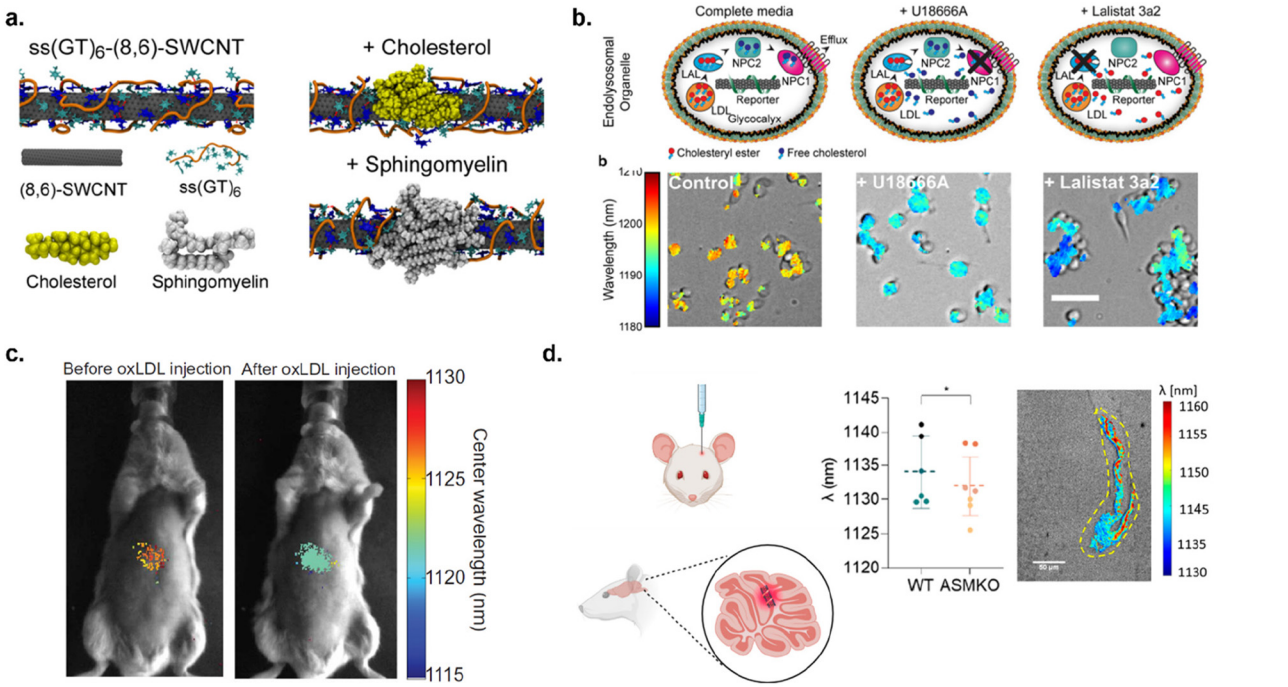

Fig. 10 Detection of lipid accumulation in cells and mouse models. (a) MD simulation snapshot of (8,6) SWCNTs functionalized with ss(GT)$_6$ and adsorption of cholesterol and sphingomyelin onto the sensor surface. (b) Detection of lipid accumulation in cells. Schematics represent lipid accumulation in cells based on inhibition of NPC1 with treatment of U1866A and inhibition of LAL with treatment of Lalistat 3a2. Hyperspectral imaging indicates sensor response to lipid accumulation in cells based on the specified treatment.[71] (c) Hyperspectral image of ssCTTC$_3$TTC – (9,4) SWCNTs response to lipid accumulation of oxidized LDL (oxLDL) *in vivo*.[109] Reprinted with permission from ref. 109. Copyright 2018 The American Association for the Advancement of Science. (d) Schematic of injecting ssCTTC$_3$TTC – (9,4) SWCNTs into mouse brain tissue and hyperspectral imaging demonstrating wavelength shift of SWCNTs due to lipid accumulation in brain tissue. Yellow dotted lines indicate injection site.[110] Reprinted with permission from ref. 110. Copyright 2023 American Chemical Society.

fluorescence and the mechanism has been determined *via* redox reactions.[112] Jin *et al.* developed a sensor array consisting of collagen functionalized SWCNTs incorporated into a thin film for monitoring H_2O_2 flux from epidermal growth factor receptor (EGFR).[113] EGF is expressed in epidermal carcinoma cells, and when activated by EGFR, H_2O_2 is produced. The nanotubes responded to the generation of hydrogen peroxide in real-time *via* quenching of nanotube fluorescence. Bhattacharya *et al.* sought to use H_2O_2 signals as a technique for evaluating chemotherapeutic efficacy in pancreatic ductal adenocarcinoma cells (PDAC).[114] Treatment of PDAC with chemotherapeutic drugs (gemcitabine and irinotecan) produce H_2O_2 during their cytotoxic activity.[114] Monitoring the real-time production of H_2O_2 from treatment with chemotherapeutic drugs could be related to tumor cell cytotoxicity and ultimately therapeutic efficacy. SWCNTs were functionalized with ssDNA, $(GT)_{15}$, a sequence that is known to detect H_2O_2.[115] $(GT)_{15}$-SWCNTs were used for monitoring differences of H_2O_2 produced from PDACs after treatment with these chemotherapeutic drugs *in vitro* and *in vivo*. As SWCNTs exhibit characteristic Raman and PL signals which could be sensitive to changes in their local environment, both Raman and photoluminescence measurements were utilized as dual signals to evaluate the sensor response towards H_2O_2. Prior study has shown that PL on DNA-SWCNTs decrease upon introduction of hydrogen peroxide. This type of optical response has been mainly described as reversible charge-transfer quenching upon H_2O_2–SWCNT contact caused by hydrogen peroxide's high reduction potential. Furthermore, absorbance of SWCNT also decreased in response to hydrogen peroxide addition unraveling the effects of hydrogen peroxide on SWCNT optical transitions. Since resonant Raman peak intensities couple to optical transitions, Raman intensity could also decrease with H_2O_2. In fact, the DNA-SWCNT hybrids showed reversible alternation in Raman and PL properties in response to hydrogen peroxide level. Thus, both Raman and PL effects could be used for detecting hydrogen peroxide. Additionally, a confocal Raman microscope, which was also equipped to record PL spectra and Raman spectra was used for *in vitro* studies to gain insights on spatial distribution of hydrogen peroxide production inside cells. *In vitro* experiments revealed monotonic quenching of fluorescence and Raman signals with increasing H_2O_2 concentrations. *In vivo* experiments consisted of implanting the sensor in live mice presenting pancreatic tumors *via* creating a well inside the tumor and delivering sensor into the well. The sensor was secured inside the tumor with biological glue. After implantation, the tumors were treated with gemcitabine to induce H_2O_2 production. This led to a 50% decrease in

the Raman G-band signals when compared to the untreated tumor. The Raman signals of SWCNTs were found to be reversibly recovered in gemcitabine-treated mice upon recovery from the influence of the drug treatment. This technique could be expanded to evaluate the efficacy of other chemotherapeutic drugs.

Monitoring enzyme activities

Enzymes facilitate biochemical reactions in the body and are important for respiration, digestion, muscle, and nerve functions.[116] However, enzyme imbalance can lead to adverse human health impacts including metabolic diseases, neurodegenerative diseases, and cancer.[117–119] SWCNT-based sensors have been developed for monitoring enzymatic reactions in real-time.[120] Loewenthal *et al.* developed SWCNT-based nanosensors for monitoring cholinesterase activity and inhibition.[121] A library of DNA-SWCNTs with varying DNA sequences was exposed to enzymatic reaction which involved acetylcholinesterase (AChE) and its substrate acetylthiocholine to identify optimal DNA-SWCNT complexes that facilitate monitoring the enzymatic reactions. It was found that $(GT)_{15}$ – SWCNTs and $(T)_{30}$ – SWCNTs specifically responded to thiocholine, the hydrolyzed product of acetylthiocholine, *via* increases of ~50% and 70% nanotube fluorescence respectively. The LOD was 10^{-3}–10^{1} U L^{-1} in serum. It was proposed that DNA conformational changes on the nanotube surface during recognition of thiocholine could trigger an optical response from nanotubes most likely due to solvatochromism. Whereas the other DNA-SWCNTs tested had a smaller and/or nonspecific response. The sensors were then immobilized on a coverslip and thiocholine was detected through single-molecule sensor event (individual DNA-SWCNTs) *via* spatiotemporal fluorescence imaging. Furthermore, the presence of neostigimine, a cholinesterase inhibitor, was distinguished *via* diminished fluorescence response by more than three times less compared to uninhibited enzyme. Basu *et al.* functionalized SWCNTs with myristocholine (MC), a natural substrate of cholinesterase (ChE), for the direct detection of ChE in blood plasma.[122] It was hypothesized that the hydrolysis of MC *via* ChE would produce choline thereby inducing fluorescence signal changes from the nanotube sensor. Upon addition of 5.05 U L^{-1} ChE, a dose-dependent quenching in nanotube fluorescence was observed up to three hours after ChE addition. This response correlated to the amount of choline molecules produced from MC hydrolysis. Therefore, the hydrolysis of MC by ChE could have induced conformational changes on the nanotube surface inducing fluorescence modulation. The presence of ChE inhibitors in blood plasma was determined by the unvaried fluorescence signal revealing the absence of choline production. Thus, these two studies show promising results on nanotube-based technologies for monitoring enzyme activities in biofluids.

SWCNTs can be used to enhance biochemical assays. Current methods for monitoring enzymatic reactions include enzyme-linked immunosorbent assays (ELISAs) and western blots, which often utilize enzymatic reactions to quantify concentrations of an analyte *via* visible color change.[123,124] Thus, the sensitivity of these techniques is limited to the visible wavelength spectrum. Metternich *et al.* designed nanosensors for overcoming limitations of ELISAs and western blots.[125] Since SWCNTs are highly sensitive to their local physicochemical environment, these materials could be used to enhance the sensitivity of the current methods to lower concentrations of analyte. This study utilized phospholipid-polyethylene glycol (PEG-PL) and short sequence DNAs to functionalize nanotubes and used these nanotube complexes to identify their sensitivity towards β-galactosidase and horse radish peroxidase (HRP) substrates/products. For HRP study, the sensor was incubated in the presence of HRP, its substrate *p*-phenylenediamine (PPD), and reaction product Bandrowski's base (BB). Sensors for β-galactosidase sensitivity were incubated with β-galactosidase and their respective substrates. The HRP sensors responded to PPD and BB with nearly 164% fluorescence increase and about 87% fluorescence decrease respectively. It was hypothesized that the enzymatic reactions would cause DNA conformational changes thereby inducing fluorescence changes from the nanotubes. Additionally, the sensor's detection limit was 50× lower in concentration of BB compared to the traditional visible readout. DNA-SWCNTs tested with β-galactosidase had lesser response. Furthermore, there was a non-linear dependency between the visible and NIR readouts which was attributed to the affinity of the substrate/product to the nanosensor. This was called sensor-based signal amplification and translation.[125] The signal enhancement of DNA-SWCNTs in response to HRP substrate showed an increase up to 120× compared to the visible absorption signal. Thus, the substantial signal enhancement using SWCNTs for NIR readouts in monitoring enzymatic reactions *in vitro* could help enhance the sensitivity of current biochemical assays for analyte detection.

SWCNT-based optical sensors for plant health monitoring

The increasing world population has necessitated the need for smart agriculture to ensure adequate food supply. To prevent the crops from damage, early detection of plant stresses and diseases is crucial so that timely interventions can take place. Wu *et al.* developed nanosensors for monitoring of hydrogen peroxide, a key signaling molecule associated with the onset of environmental stress in plants.[73] Early detection of environmental stress within the plant can lead to early action to prevent further damage to the crop.[73] SWCNTs were functionalized with DNA aptamer that bind to hemin. Hemin binds to ferric iron and undergoes a Fenton-like reaction with hydrogen peroxide. Nanosensors were infiltrated into plant leaves by applying the nanosensor solution to the underside of the leaf *via* gently pressing a syringe against the leaf lamina.[73,126] It was shown that this optical nanosensor can detect hydrogen peroxide within the plant physiological range of 10–100 μM.[73] Therefore, the infiltration of SWCNTs into plant leaves seems to be a viable method for monitoring plant stress *in vivo*. Another approach for early detection of plant stress could be monitoring plant metabolites associated with defense mechanisms. Nißler *et al.* reported an array of sensors functionalized

with ssDNA and PEG-PL polymers for the detection of polyphenols, a class of metabolites that are involved in plant defense mechanisms against pathogens and herbivores.[127] There is a general tendency of fluorescence increase for ssDNA–SWCNTs and a decrease for PEG–PL–SWCNTs. Tannic acid, a structurally large polyphenol, was used as a model compound to study the interaction between tannins and the sensors. With ssDNA–SWCNTs, PL intensity increased in nM regime and decreased in the μM to mM range. Such PL changes in DNA-SWCNTs could be explained based on antioxidant effects of polyphenols at lower concentration (nM) and aggregation effects at higher concentration. However, PEG–PL–SWCNTs showed a consistent decrease in the PL intensity with polyphenols. It was observed that the PEG-PL-SWCNTs can respond to polyphenols within the 0–10 μg mL^{-1} range in plant tissue and culture medium by exhibiting a significant red-shift and decrease in nanotube fluorescence. Furthermore, E_{11} absorption maximum of PEG–PL–SWCNTs was red-shifted by approximately 10 nm. The decrease in PL intensity and red-shifting phenomenon could not be simply explained by classical antioxidant effects of polyphenols. It was hypothesized that the strong interaction between the sensor and the polyphenol analyte could cause changes in solvation effecting exciton diffusion along the nanotube surface. Furthermore, *in situ* detection was enabled by allowing soybean seedlings to grow on the agar medium that contained embedded sensors. The soybean roots were then exposed to an elicitor that would cause polyphenol production from the embryonic (Fig. 11a). The sensor response to polyphenol production was determined with an NIR stand-off imaging system over a 24-hour period. The results showed that the NIR signal decreased close to the elicitor-induced area where increased polyphenol secretion was observed within the first 4–8 h then stabilized over the remaining 24 h of the experiment (Fig. 11b).[127] This allowed for direct real-time monitoring of polyphenol production in plant root systems.

Phytohormones are considered biomarkers for plant stresses. Gibberellins (GA) are plant hormones that regulate various developmental processes, including stem elongation, germination, dormancy, flowering, flower development, and leaf and fruit senescence.[128] Plant stress alters GA expression in the root system thereby effecting plant growth. Thus, monitoring changes in GA expression could aid in early detection of plant stresses. Boonyaves *et al.* developed nanosensors for the detection of gibberellins (GA)[129] (Fig. 11c). This study employed CoPhMoRe techniques to identify a sensor that had sensitivity towards GA molecules. Polymers were custom designed to facilitate hydrogen bonds with GA while adsorbing to SWCNTs to provide colloidal stability. After library screening, two corona phases were identified to have affinity towards two types of GA compounds with an LOD of 542 nM and 2.96 μM to GA_3 and GA_4 in buffer solution.[129] This affinity was most likely due to a combination of electrostatic interactions, hydrogen bonding, and steric interactions between the polymer on

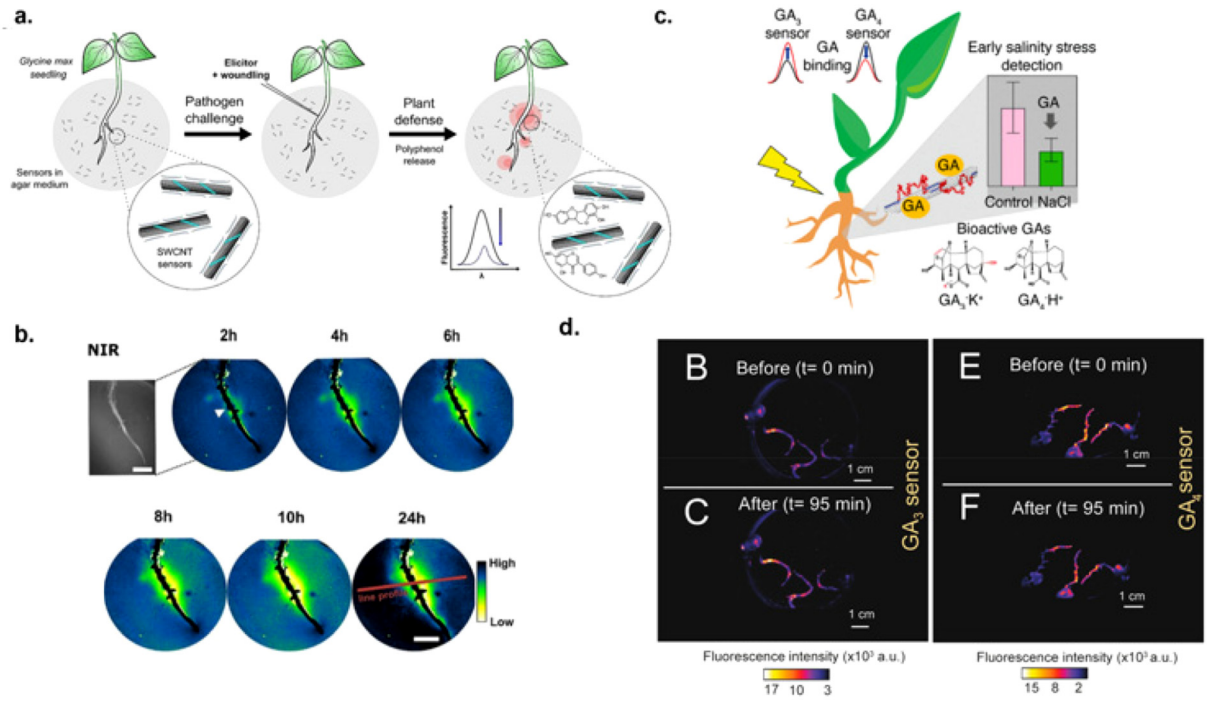

Fig. 11 Monitoring plant health *in vivo*. (a) Schematic of PEG-PL-SWCNTs detection of polyphenols in agar medium with plant seedling.[127] (b) NIR fluorescence images of sensors responding to pathogen-induced generation of polyphenols over 24 hours. The white triangle indicates point of wounding, red line indicates line position, scale bar is 1 μM.[127] (c) Schematic of SWCNT detection of gibberellins hormones (GA_3 and GA_4) in plant roots under salinity stress.[129] (d) NIR fluorescence images of GA_3 (i–ii) and GA_4 (iii–iv) sensors before (t = 0) and after exposure (t = 95 min) to 100 μM of GA_3 and GA_4 respectively.[129] Reprinted with permission from ref. 129. Copyright 2023 American Chemical Society.

SWCNT and GA compounds. Binding of the analyte to the sensor could cause dielectric environment changes in the proximity of the SWCNT resulting in solvatochromic shifts. Once *in vitro* functionality was established, *in vivo* capabilities were tested by infiltrating the roots of basil and *Arabidopsis* seedlings by incubating the seedlings in SWCNT-sensor solution overnight. The seedlings were then immersed in 100 μM of GA and the sensors exhibited maximum fluorescence changes within 95 minutes of exposure (Fig. 11d). Additionally, GA dynamics were monitored in *Arabidopsis* plants by developing a NIR/Raman fluorimeter to eliminate the need for a reference sensor, thus expediting data collection. This instrument utilized the Raman G-band in SWCNTs to be used as an internal reference in which the Raman signal would remain unvaried in the presence of specific and non-specific molecules. The accumulation and depletion of GA in *Arabidopsis* plants overexpressing GA or under salinity stress was detected. This provides a new method/technology to study GA dynamics in plants.

Detection of bio-electrolyte metal ion, heavy metals and other contaminants

SWCNT-based sensors have been used to detect contaminants in water,[130] fish tissues,[131] and model biofluids.[132] Exposure to heavy metals such as Cd^{2+}, Pb^{2+}, Fe^{2+}, Hg^{2+}, Zn^{2+}, and Cu^{2+} present in water can cause health issues including neurodegenerative diseases and cancer.[133,134] Wulf *et al.* developed SWCNT-based optical sensors using a melanin inspired polymer to functionalize SWCNTs for the detection and scavenging of metals ions from aqueous sources.[130] The polymer contained catechol and *ortho*-quinone functional groups to facilitate binding of metal ions. Of the metal ions tested, a dose-dependent increase/decrease in nanotube fluorescence was observed with Fe^{2+}/Cu^{2+} with concentrations ranging from 0–100 μM for Fe^{2+} and 0–1.24 μM for Cu^{2+}.[130] Additionally, LODs ranged from 19–413 nM for all metal ions tested. The accumulation of metal ions close to the nanotube surface would likely change the dielectric environment thereby inducing fluorescence changes. Gong *et al.* developed sensors for divalent metal ion detection *via* CoPhMoRe methodology using DNA-SWCNTs.[131] Through the optimization of several experimental parameters, the authors developed a protocol for optimal sensing with DNA-SWCNTs. By using these parameters, it was shown that DNA-SWCNT corona phases can differentiate between Mn^{2+}, Hg^{2+}, Cr^{2+}, and Pb^{2+} in buffer. Furthermore, these sensors were applied for detection of Hg^{2+} in fish tissue *via* portable NIR reader and a paper-based barcode strip. The nanosensors were deposited onto the substrate and exposed to fish tissue extract spiked with mercury salts to increase concentration of Hg^{2+}. The sensors detected 33 nM of Hg^{2+}, which is much lower level compared to the average mercury content in fish tissues (~1.1 μM).[131] Therefore, these sensors could be employed for monitoring heavy metals for food safety applications. Besides heavy metals, functionalized carbon nanotubes could be employed as optical reporters for the detection of potassium ion, a key electrolyte that plays vital role in cardiovascular, ocular and neurological health. Dewey *et al.* reported optical detection of potassium ions in simulated biofluids using SWCNT-based sensors.[176] SWCNTs were non-covalently functionalized with polystyrene sulfonate, FDA approved polymer to treat hyperkalemia, and its derivative to allow effective interaction between potassium ion and the nanosensor. The nanosensor showed a dose-dependent optical response to potassium ions *via* PL increase. The fluorescence changes was attributed to solvatochromic changes due to ion exchange and water molecules displacements from nanotube proximity. The optical response was distinct within 5 minutes of exposure and a limit of detection was 0.39 mM potassium chloride solution.[176]

The increased use of quaternary ammonium compounds (QACs), an active ingredient in chemical disinfectants, during the COVID-19 pandemic has caused increases in human exposure to these chemicals. Furthermore, QACs have been associated with adverse health impacts including increase in inflammatory cytokines, decrease in mitochondrial function, and disruption of cholesterol homeostasis.[135] Recent reports show that QACs can appear in human milk and blood indicating these compounds can cross physiological barriers.[136] Thus, sensing technologies could aid to better understand the long-term fate and human health impacts of these compounds. Dewey *et al.* developed nanosensors using bile salts functionalized SWCNTs. For the study, the authors functionalized SWCNTs with anionic bile salt derivative, sodium cholate (SC) and zwitterionic bile salt derivative, 3-[(3-cholamidopropyl)dimethylammonio]-1-propane sulfate (CHAPS) hydrate. These functionalized carbon nanotubes were used for the detection of QACs in serum media.[132] Dose-dependent increases in nanotube fluorescence were observed within minutes of addition of QACs. The LOD for detection of benzalkonium chloride (BAC), a commonly used QAC, was 0.68 nM.[132] The detection range was within the concentration range of BAC that was found in human blood samples during pandemics. The sensing mechanism was attributed to solvatochromic and dielectric changes due to lipophilic and electrostatic interactions between BACs and the nanosensor, causing water displacement away from the nanotube surface. Since BAC is a commonly used QAC in many household cleaners and chemical disinfectants, this affinity was advantageous for future applications in biofluid analysis to gain insights on exposure and associated health impacts.

Portable and wearable sensing platforms

While there has been increasing interest in the development of SWCNT-based optical nanosensors, rendering them into a portable matrix while maintaining sensor functionality remains a challenge. This is due to SWCNTs extreme sensitivity to their surrounding environment.[64,68] Budhathoki-Uprety *et al.* addressed this challenge by incorporating their SWCNT-based sensor into an acrylic paint matrix (Fig. 12a).[64] It was reported that the sensor response was consistent in solution and when embedded within the polymer matrix in

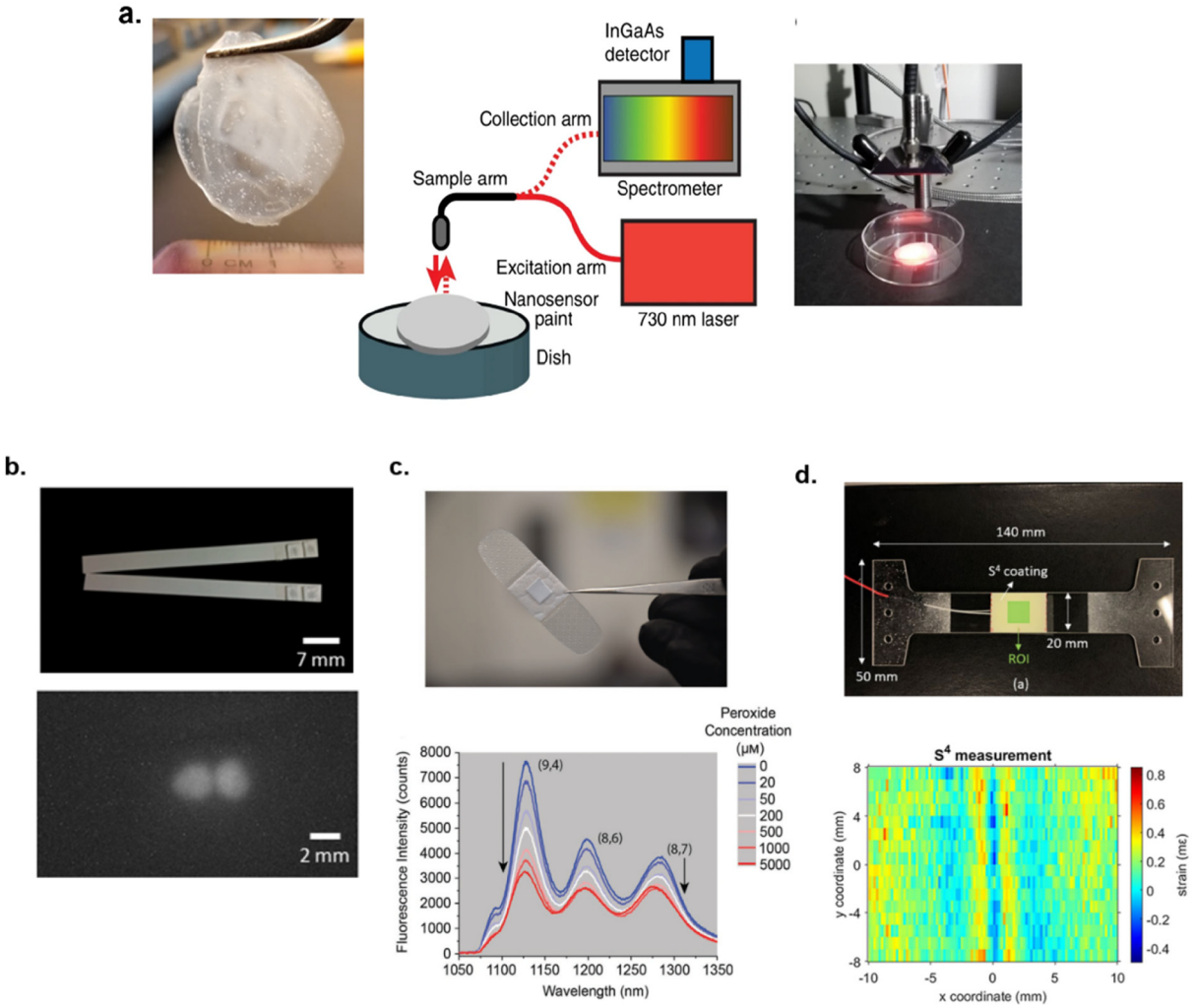

Fig. 12 SWCNTs incorporated into portable and wearable platforms. (a) Photograph of polycarbodiimide-SWCNTs in acrylic paint matrix. Sensors retained response to albumin in urine samples.[64] The schematic shows measuring the sensor response using fiber-optic probe. Reprinted with permission from ref. 64. Copyright 2019 Springer Nature. (b) Peptide-SWCNTs on paper substrate and their NIR fluorescent response to trypsin.[137] (c) ssDNA–SWCNTs in fibrous matrix adhered to wound bandage for detection of hydrogen peroxide. SWCNTs in fibrous matrix responded to increasing concentrations of hydrogen peroxide *via* quenching of nanotube fluorescence.[70] Reprinted with permission from ref. 70. Copyright 2021 John Wiley and Sons. (d) Sensors incorporated into strain-sensing smart skin on an acrylic substrate and their strain-induced NIR response.[138]

solid state.[64] Furthermore data acquisition could be performed using a probe-based system as illustrated in Fig. 12a. Shumeiko *et al.* utilized peptide-SWCNTs immobilized on a paper-based substrate for the portable detection of protease activity (Fig. 12b).[137] The sensor was drop-casted onto the paper substrate and adhered to a dipstick which could be dipped into protease solution. The sensor exhibited a decreased fluorescence in nanotube emissions in response to trypsin (a serine protease) in urine at concentrations ranging from 1–20 μg mL^{-1}. This concentration range was relative to acute pancreatitis. Safaee *et al.* developed core–shell nanofibers comprising ssDNA–SWCNTs, poly(ethylene oxide), and poly(caprolactone) PCL to enable a portable and wearable SWCNT-based nanosensor for the real-time monitoring of hydrogen peroxide.[70] The $(GT)_{15}$ – SWCNTs that were previously shown to exhibit optical responses to hydrogen peroxide, retained their sensing capability within the nanofiber matrix and when the nanofibers were adhered to a wound bandage (Fig. 12c).[70] This demonstrates the potential of wearable nanosensors for personal health monitoring. Meng *et al.* developed a strain-sensing smart skin (S^4) consisting of poly (9,9-di-*n*-octylfluorenyl-2,7-diyl) (PFO) wrapped SWCNTs for monitoring strain to mitigate structural failures in materials used in buildings, bridges, aircraft, *etc.*[138]

The nanotubes were suspended in organic solvent and applied to specimen substrate. To prevent degradation of the substrate by the organic solvent, a blocking layer and polyurethane layer were added in between the substrate and the S^4. Acrylic, concrete, and aluminum substrates were subjected to strain and NIR emissions from the nanotubes were recorded as a color-coded strain map (Fig. 12d). The sensors enabled direct measurement of strain in each of the materials tested.

Thus, SWCNT-based sensors can be used for monitoring structural health.

SWCNT sensors embedded into hydrogels matrixes

SWCNT-based sensors have been integrated into hydrogel matrices for portable and implantable applications. Hydrogels are three-dimensional polymer networks that are synthesized *via* cross-linking of hydrophilic polymers that can retain water within their network without compromising the structure.[139] Natural (polysaccharides, collagen, lignin, nucleic acids) and synthetic polymers (polyethylene glycol, polyethylene oxide, poly(lactic acid), poly(vinyl alcohol))[140] have been used to create hydrogels that can respond to different stimuli and mimic extracellular matrices.[141,142] This is advantageous for biomedical applications such as tissue engineering, cell culture, and biosensing. Thus, SWCNTs embedded into hydrogels could provide a vehicle to impart biocompatibility for implantable applications. Barone *et al.* first characterized SWCNTs fluorescent response within poly(vinyl alcohol), PVA hydrogel matrices.[143] They observed a red-shifting and decreasing in nanotube fluorescence with increasing cross-linking density. Furthermore, a reversible photoluminescence shift from the nanotubes was observed with change in hydration state of the hydrogel from wet to dry. This was most likely due to changes in the dielectric environment surrounding the nanotube as cross-linking densities and hydration states varied. To test the functionality of the sensor *in vivo*, apoglucose oxidase, an enzyme that converts glucose into oxygen, was chemically attached to the PVA hydrogel for molecular recognition of glucose. The hydrogel-sensor was then implanted subdermal in a mouse model and exposed to 10 mM of glucose. NIR fluorescence measurements of the hydrogel-sensor were taken *via* NIR fluorescence microscope. NIR measurements showed that the PVA encapsulated nanotubes retained their response to glucose *in vivo* following implantation.[143] This study demonstrated that SWCNT sensors incorporated into hydrogel matrix could maintain sensing functionality *in vivo*. Since then, researchers have utilized hydrogels as implantable and injectable sensing materials for *in vivo* sensing and imaging applications.[81,144–146] Iverson *et al.* investigated performance optimization of SWCNTs encapsulated in a hydrogel matrix for *in vivo* monitoring applications.[144] ssDNA–SWCNTs were encapsulated into alginate and PEG hydrogels *via* mixing the nanotubes in alginate or PEG solution and cross-linked using chemical agents or UV light respectively. The performance of the hydrogel-sensor in tissue was evaluated *via* implantation into chicken breast as a model animal tissue and the nanotubes were imaged *via* NIR microscope. The results showed a detection limit of 5.4 mm and 5.1 mm in tissue depth for alginate and PEG hydrogels, a nanotube concentration of 10 mg L^{-1}, laser excitation of 785 nm at 80 mW, and 30 seconds exposure for optimal imaging in animal tissue.[144] Lee *et al.* demonstrated *in vivo* functionality of SWCNT-based progesterone sensor embedded within PEG hydrogels.[81] Nißler *et al.* developed sensors for remote detection of pathogens *via* encapsulating DNA-SWCNTs within porous polyethylene glycol diacrylate hydrogels.[86] The porosity of the hydrogels was varied to allow for diffusion of target molecules and prevent nonspecific interactions. For example, smaller pore sizes were created in sensors for targeting siderophores whereas hydrogels with high porosity allowed for sensor interactions with larger enzymes for detection of virulence factors associated with *Streptomyces griseus* and *S. aureus*. $(GT)_{15}$-SWCNT-hydrogel injectables were used to monitor doxorubicin, a chemotherapeutic drug, in mice.[145] Typical implantation procedures involve surgically implanting SWCNTs in dialysis bags or hydrogels into animal tissue by subjecting the animal model to anesthesia, making an incision at the target site, and monitoring the wound healing process.[81,84,114] Cohen *et al.* sought to mitigate surgical procedures involved in implantation to achieve truly noninvasive biosensing.[145] $(GT)_{15}$-SWCNTs were incorporated into methacrylated methylcellulose (MC) based hydrogels for doxorubicin detection. MC was dissolved in buffer solution containing $(GT)_{15}$-SWCNTs, cross-linked using redox initiators, then extruded using a mixing tip. The SWCNT-gels were implanted subcutaneously *via* dorsal injection into mice. Nanotubes responded to doxorubicin *via* red-shifting in their fluorescence and the optical signals were discernable up to two months after injection. Thus, injectable SWCNT-sensor hydrogels are shown to be a viable option for noninvasive implantation procedures. Researchers have also used SWCNT sensors to monitor structural and morphological changes in hydrogels. For example, peptide hydrogels can self-assemble into fibrillary structures that mimic extracellular matrices, and thus have found applications in tissue engineering, repair, and wound healing.[147,148] Each application requires different hydrogel structural properties and morphologies. Furthermore, the stability of hydrogels is highly dependent on the manufacturing process.[149] Thus, monitoring changes in the hydrogel structure is crucial during tissue repair and wound healing processes. However, current characterization techniques do not give real-time information of changes in the hydrogel structure during their use in biological environments. Wulf and Bisker addressed this by studying the self-assembly of peptide hydrogels in real-time.[149] In this study, SWCNTs were functionalized with fluorenylmethyloxycarbonyl-diphenylalanine (FmocFF), a peptide conjugated with amino acid commonly used to form hydrogels, and the nanotubes were incorporated into hydrogels.[149] Additionally, dextran, polyethylene glycol, and sodium alginate, polymers commonly used as additives to tune the structural and morphological properties of hydrogels, were added to the FmocFF-SWCNTs-FmocFF hydrogels. The FmocFF-SWCNTs were used as probes to characterize structural and morphological properties during gelation in real-time *via* NIR microscope.[149] It was reported that structural changes from FmocFF/polyethylene glycol hydrogels during self-assembly had the largest fluorescence signals from the nanotubes where signals decreased down to 60% and red-shifted up to 6 nm. These shifts were attributed to the polymer arrangement close to the nanotube surface caused changes in the nanotube's dielectric

environment. The use of SWCNTs as optical probes for characterization of hydrogels could yield applications in tissue engineering, cell culture, and biosensing.

While many studies have utilized hydrogels for portable and implantable sensing applications, it is important to characterize the behavior of these materials in biological systems. Lee *et al.* studied inflammation and foreign body response of SWCNTs in hydrogels consisting of polyethylene glycol diacrylate (PEGDA).[150] After implantation of SWCNT sensor-hydrogels into mice, tissue responses were tracked, and the degradation of the hydrogels was characterized. It was observed that higher cross-linking density in hydrogel formulations helped to contain SWCNTs within the hydrogel matrix, mitigating from leaking out of the hydrogel. Additionally, greater cross-linking density allowed for reduced inflammation responses and faster inflammation resolution. This was hypothesized to be due to smaller pore sizes within the hydrogel allowing for better encapsulation of the nanotubes. Furthermore, degradation of gel matrix products and leakage of nanotubes were not detectable with gel permeation chromatography or Raman spectroscopy when the experiments were conducted in buffer solution. Additionally, ss$(AAAT)_7$ wrapped SWCNTs in hydrogel led to reduced inflammation responses as compared to polymer, p(acrylic $acid_{54}$-*ran*-$styrene_{22}$-*ran*-$acrylated\ cortisol_4$), wrapped nanotubes. Classical wound healing processes including neutrophil density, fusion of macrophages, and formation of a fibrous capsule around the hydrogel were monitored after implantation. Masson's trichome staining of the implant revealed the beginning of fibrous capsule formation at day 7 and complete encapsulation 28 days after implantation.[150] This study outlined the importance of SWCNT wrappings and cross-linking density in SWCNT-hydrogel formulation to yield desired outcomes for *in vivo* applications.

Organic color center (OCC)-based SWCNT sensors

The OCC-SWCNTs have been explored as sensors for detection of biomolecules which include neurotransmitters, proteins, bacteria, and sugar molecules. Spreinat *et al.* exploited sp3 quantum defects to understand sensing mechanisms of dopamine detection.[151] To gain insights on how quantum defects could affect SWCNT optical sensing, the responses of non-defect ssDNA–SWCNTs were compared with ssDNA–SWCNTs with low NO_2-aryl defects. The results showed that while non-defect ssDNA–SWCNTs showed a 250% fluorescence increase in response to 100 μM of dopamine, the defect ssDNA–SWCNTs exhibited a decreased emission by 35% and 50% in the original E_{11} and defect E_{11}^* respectively.[151] This signal reversal was attributed to a combination of decreased non-radiative decay rate, increased exciton diffusion, and increased non-radiative decay rate of defect state explained by a Monte Carlo simulation studies of exciton diffusion, which supported a change in two non-radiative decay pathways together with an increase in exciton diffusion (three-rate constant model).[151] Authors used quantum defect-SWCNTs for ratiometric sensing of dopamine utilizing responses at two different emission wavelength corresponding to non-defect and defect sites. Shiraki *et al.* introduced sp^3 defects on SWCNTs *via* anchoring phenylboronic acid groups (PB) on nanotube surface for the detection of sugar molecules.[152] These PB-SWCNTs were developed through diazotization of 4-aminophenyl boronic acid pinacol ester, an aryldiazonium derivative with PB groups, and mixing them with SWCNTs dispersed with SDBS. Upon addition of 0–19 mM D-fructose to PB-SWCNTs in solution, a blue-shift of the E_{11}^* peak was reported.[152] It was suggested that PL modulation was due to electronic property changes within the PB moiety upon recognition of D-fructose at the chemically modified sites on the tubes (Fig. 13a). Metternich *et al.* established a defect-induced covalent functionalization approach by anchoring a guanine-containing ssDNA sequence, $(GT)_{15}$, to the SWCNT surface.[153] Covalent attachment was achieved by incubating non-covalently functionalized ssDNA–SWCNTs with rose bengal to induce the production of singlet oxygens thereby covalently attaching guanine bases to the SWCNT lattice.[153] Anchoring ssDNA to the nanotube surface was utilized to prevent non-specific movement of the DNA corona on the nanotubes. It was hypothesized that mitigation of unspecific changes in DNA arrangement would provide precise optical responses during molecular recognition.[153] In addition, non-guanine containing aptamers were attached to the capture sequence for recognition of bacterial siderophores and SARS-CoV-2 spike protein in DNA-SWCNTs (Fig. 13b). The nanotubes functionalized with aptamer, which could recognize bacterial siderophores, showed an optical response with a nanotube fluorescence increase upon addition of bacterial siderophores – deferoxamine B (DFO) and pyoverdine up to 75% and 83% respectively. The SARS-CoV-2 spike protein aptamer functionalized nanotubes showed response *via* nanotube fluorescence decrease by 10%.[153] Furthermore, these guanine-defects-SWCNTs retained their specific responses in serum media, demonstrating sp^3-defect induced SWCNTs as promising nanosensors. Shiraki, Fugigaya and Goto research groups chemically-modified SWCNTs with luminescent defects to establish a correlation between the E_{11}^* PL energy shift and the induction-polarity parameters of surrounding solvents and for detection of avidin proteins. To facilitate interactions with these avidin proteins, biotin moieties were covalently attached to SWCNTs *via* diazonium chemistry followed by post-modification.

Upon addition of neutravidin to the functionalized-SWCNTs, nanotube's emission wavelength red-shifted which was attributed to an increase in the induction-polarity parameters around the biotin-doped sites due to the adsorption of neutravidin onto the SWCNTs.[154] PL changes were noticeably distinct with neutravidin when responses were compared to that of avidin and streptavidin. Thus, the PL peaks shift was attributed to the structural differences of avidin protein derivatives (neutravidin, streptavidin and avidin) adsorbed on the biotin-functionalized SWCNTs *via* avidin–biotin interactions at

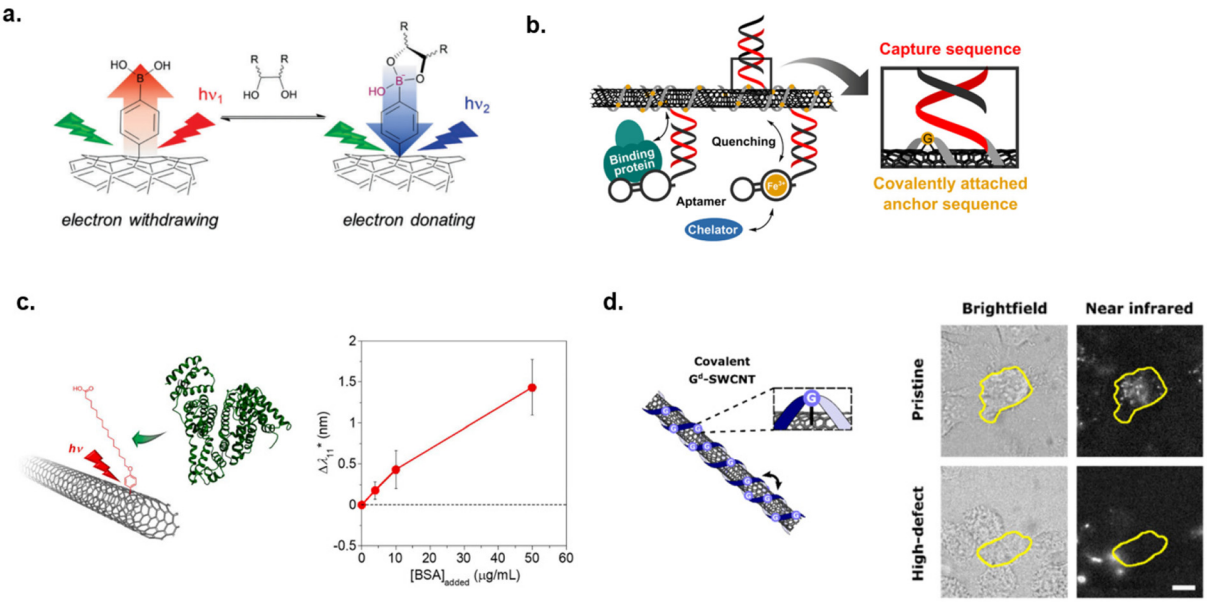

Fig. 13 . Organic color center-based SWCNTs sensors. (a) Molecular recognition of sugar molecule with phenylboronic acid (PB)-functionalized sp^3 defect-SWCNTs. The electron withdrawing/donating properties change as interactions with PB-SWCNTs form boronate with a diol compound.[152] (b) Guanine-defect induced SWCNTs with a capture sequence for recognition of bacterial siderophores and SARS-CoV-2 spike protein.[153] Reprinted with permission from ref. 153. Copyright 2023 American Chemical Society. (c) Detection of albumin protein with defect-SWCNTs functionalized with palmitic acid.[155] Reprinted with permission from ref. 155 Copyright 2024 Elsevier. (d) SWCNTs with covalently attached $(GT)_{10}$ for detection of dopamine and monitoring of cellular uptake.[156] Defect-SWCNTs increased fluorescence in response to dopamine. NIR fluorescence images show cellular uptake between non-defect and high defect SWCNTs.[156] Reprinted with permission from ref. 156. Copyright 2021 American Chemical Society.

the doped sites of the nanotubes.[154] Furthermore, the nanotubes were immobilized in a 3-aminopropyltriethoxysilane (APTES)-treated quartz substrate to create insoluble SWCNT film devices and to enhance sensor responsiveness. Upon immersion into streptavidin solutions ranging, the PL intensity decreased with increasing concentration. Additionally, Niidome *et al.* utilized OCC-SWCNTs to enable detection of albumin protein in serum. Albumin, the most abundant serum protein, is a fatty acid transporter and hence, could bind to fatty acids on the nanotubes. The authors functionalized sp^3 defect sites on SWCNTs with palmitic acid (fatty acid) for the detection of albumin protein[155] (Fig. 13c). A red-shifting in nanotube fluorescence up to 2.5 nm, 2.1 nm and 1.8 nm was observed in the presence of 100 μg mL^{-1} of each bovine serum albumin (BSA), human serum albumin and mouse serum albumin respectively in buffer solution. The fluorescence changes on the nanotubes was ascribed due to increased dielectric environment induced from interactions between albumin and palmitic acid. Control experiments showed nanotube emission changes at much lesser degrees ranging from 0.5 nm to 1.1 nm. Examples included use of nanotubes that did not contain a fatty acid functional group or use of proteins other than albumin (*i.e.*, ovalbumin). Furthermore, the sensor was tested in serum and urine samples diluted in PBS buffer for potential use in clinical and biological applications. A red-shifting of 1.4 nm at 50 μg mL^{-1} of BSA-spiked in fetal bovine serum samples diluted in buffer was also reported (Fig. 13c). The magnitude for optical response from the nanotube sensors appears to be hindered by the presence of other proteins in the serum environment. The nanotube sensors were also tested in the urine samples from diabetic mice that showed albuminuria conditions (urine albumin excretion 200–300 μg day^{-1}). In the urine samples from diabetic mice (albumin concentration, 20 ± 11 μg mL^{-1}), the nanotubes showed up to ~4.5 nm emission shift, which was relatively larger when compared to the response from the nanotubes (emission shift, ~3.3 nm), to the control urine samples from non-diabetic mice (albumin concentration 9 ± 5 μg mL^{-1}). Although the study could be extended further to establish sensitivity, selectivity and dynamic range for detection, the results from the *in vivo* study shows promises that SWCNTs with locally functionalized sp^3 defects could be used in biofluid analysis. Galonska *et al.* utilized guanine-defect SWCNTs *via* attachment of $(GT)_{10}$ *via* guanine-cross linking chemistry on the nanotube surface and utilized guanine-defect SWCNTs as sensors for dopamine (Fig. 13d).[156] Additionally, nanosensor responses to dopamine were compared using non-covalently functionalized DNA-SWCNTs and the ones with guanine-defect SWCNTs. The sensor response to 100 μM of dopamine exhibited a fluorescence increase up 72% for guanine-defect SWCNTs whereas defect-free SWCNTs exhibited a 113% increase. Moreover, guanine-defect SWCNTs reached saturation at 1 μM compared to defect-free SWCNTs reaching saturation at 10 μM of dopamine. The lower degree of

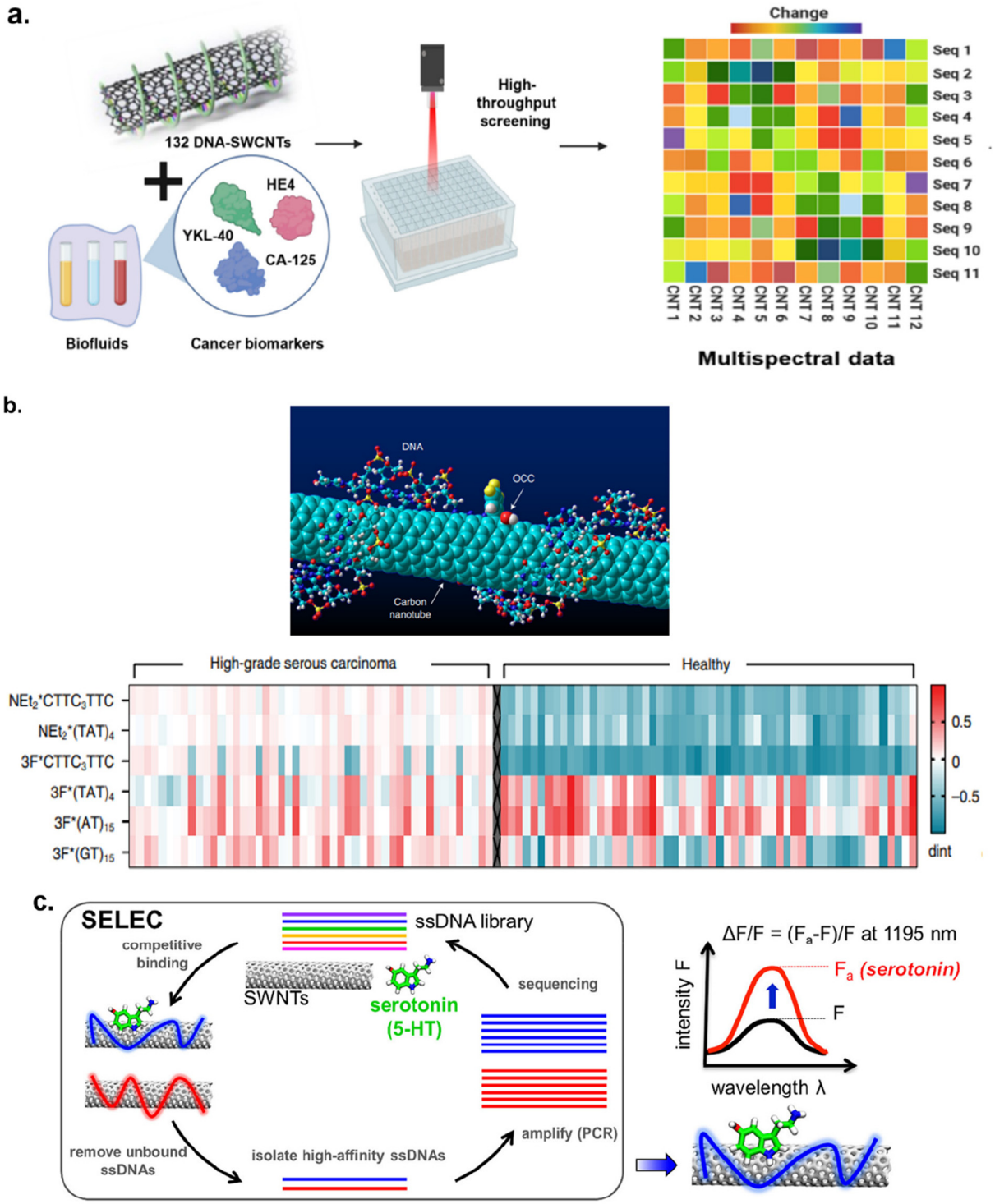

Fig. 14 Employing machine learning algorithms in SWCNT sensor development. (a) ssDNA and SWCNT combinations were analyzed *via* high throughput screening for optimal response to cancer biomarkers.[157] Machine learning algorithms predicted the best classification and quantitation outcomes. (b) OCC-DNA-SWCNT combinations were analyzed for spectral fingerprinting of ovarian cancer biomarkers *via* high throughput screening.[159] Reprinted with permission from ref. 159. Copyright 2022 Springer Nature. (c) Utilization of selection protocol, SELEC, for identification of optimal ssDNA sequence and SWCNT combination for the detection of serotonin.[161] Reprinted with permission from ref. 161. Copyright 2022 American Chemical Society.

optical response and saturation from guanine-defect SWCNTs was attributed to less flexible DNA strand on the nanotube surface causing smaller conformational changes to elicit lower optical changes in response to changes in the nanotube's surrounding environment. Furthermore, cell-based assays revealed that high defect density on SWCNTs caused a reduction in cellular uptake of nanotubes (Fig. 13d). Thus, it is important to consider the degree of defects induced on the nanotubes for cell-based analysis.

Machine learning

Recently, machine learning (ML) and perception-based strategies have been explored to enhance sensitivity and selectivity for the development of new sensors. The perception-based strategies utilizes high throughput screening (HTS) techniques involving an array of functionalized SWCNTs to characterize the target analyte through different optical responses from the nanosensor array thereby providing a spectral fingerprint of the analyte.[157,158] Then, machine learning algorithms are employed to analyze and interpret the data collected from HTS to identify and quantify the targeted analyte in various media.[157,158] Yaari *et al.* employed this technique by using ssDNA wrapped SWCNTs to detect gynecologic cancer biomarkers in biofluid (Fig. 14a).[157] High throughput NIR spectroscopy was used to measure the responses of 132 ssDNA–SWCNT complexes in the presence of ovarian and endometrial cancer protein biomarkers. The laboratory experiments included measuring optical responses (emission intensity and wavelength changes) from these various ssDNA–SWCNTs upon incubation in the presence of analytes and 10% fetal bovine serum.[157] ML algorithms enabled the classification (identifying the presence of) and quantitation of each biomarker. Furthermore, the study was expanded using clinical samples from cancer patients. Sensors were applied to uterine lavage samples obtained from cancer patients. The sensor readouts were collected, and the biomarkers were validated with ELISAs. Comparison of nanosensor results to levels detected by ELISA yielded classification of ovarian and endometrial cancer biomarkers by 100% and 91% success respectively.[157] Kim *et al.* also employed perception-based strategies for the development of SWCNT sensor array consisting of multiple types of quantum defects (OCC) and DNA wrappings for the detection of high-grade serous ovarian carcinoma (HGSOC) in cancer patient serum samples (Fig. 14b).[159] The optimal OCC-DNA combinations were determined from HTS experiments. The classification of HGSOC with support vector machine models revealed nanosensor responses with 87% sensitivity and 98% specificity, outperforming traditional serum-biomarker identification techniques.[159] Furthermore, their best performing model included spectroscopic variables that were not sensitive to known biomarkers. Interestingly, these variables had a more significant importance compared to biomarker-related ones. This revealed the importance of variables in serum samples that were not related to the known ovarian cancer biomarkers. This suggests that the nanosensor array combined with machine modeling could potentially identify the presence of new/unknown biomarkers. These studies demonstrated a new approach for the HTP detection of multiple analytes in biofluids.

Gong *et al.* utilized ML techniques to analyze various corona phases of DNA-SWCNTs as a method to improve sensor library generation for the identification of optimal CoPhMoRe and predict sensor-analyte interactions.[160] Additionally, using ML algorithms, Kelich *et al.* identified optimal DNA sequences as the recognition unit for serotonin, a neurotransmitter which is involved in the central nervous system functions.[161] ML algorithm was applied in the selective protocol called SELEC which was used to screen DNA sequences that could exhibit a high affinity to SWCNTs as well as towards serotonin (Fig. 14c). The hit sequences predicted from ML algorithm were evaluated experimentally *via* NIR spectroscopy. Interestingly, five new DNA sequences on SWCNTs showed optical responses to serotonin by almost 2-folds higher when2-fold compared to response from the previously identified sensors from experimental approach only.[161] These studies demonstrate the ability to expedite the sensor development process *via* machine learning and high throughput assays.

Conclusions and future outlook

SWCNTs possess unique optical properties that allow for NIR sensing and spectral imaging in the tissue transparent region. This advantage has led to extensive research on these materials as optical probes for the detection of target analytes in the biological and environmental sectors. The detection of various analytes has been proven in biofluid, cells, and *in vivo*. Incorporation of SWCNTs into hydrogels, fibers, and other substrates has allowed for portable, wearable, and implantable sensing applications. Moreover, the integration of artificial intelligence mechanisms has expedited sensor development and improved detection sensitivities and specificities. While studies have demonstrated numerous sensing applications, challenges still exist to translate this technology into clinical practice.

One of the challenges among nanosensor development for biomedical applications is mitigating interactions with non-specific molecules which are known to reduce targeting capability for nanoparticles.[88] Nanomaterials are often prone to non-specific molecular interactions and other macromolecules due to their hydrophobicity and large surface area.[88] This unintended protein corona formation can produce false positives, high background noise, and hindered sensor recognition/responsiveness.[88] Surface passivation techniques and encapsulation in semi-permeable membranes have been employed to address this issue.[68] Further research efforts should focus on enhancing sensitivity and specificity of SWCNT optical sensors in biological environments.

Another area for improvement involves material purification and scale-up production. Nanotube chirality purifi-

cation involves separation techniques including aqueous two-phase extraction, dielectrophoresis, density gradient centrifugation, ion exchange chromatography, gel column chromatography, and selective dispersion and extraction by polymers.[162] Efforts have also been made towards controlled growth of nanotubes to yield chirality-pure samples.[162] Nanotube purification is essential for *in vivo* applications to mitigate inflammatory responses from living organisms. However, the previously mentioned techniques are currently custom-designed and employed in labs, limiting their utilities for homogenous preparation. Future efforts could be towards developing advanced technology for single chirality nanotube production and purification. Perhaps machine learning models could be utilized in this area to expedite the process.

Although studies have incorporated SWCNT-based sensors into portable and wearable platforms, the development of a portable and sensitive NIR fluorescence spectrometer is the key for moving these research findings from the lab to clinical practices.[70,163] Studies have sought to develop miniaturized spectrometers such as Heidari-Bafroui *et al.* where a portable NIR lightbox controlled by a smartphone was made and utilized for monitoring phosphate content in water.[164] Additionally, Boonyaves *et al.* created a NIR/Raman fluorimeter to eliminate the need for a reference sensor *in vivo*.[129] Nißler *et al.* engineered a NIR stand-off detection set-up for remote imaging that could be transported between lab facilities.[86] However, most of these instruments are custom-made in a lab setting and are not widely available. These studies can serve as the basis to extend these concepts to other SWCNT-based nanosensors where portable and wearable NIR fluorescence spectrometer can transmit data *via* bluetooth to a smartphone. Thus, innovations in instrumentation and software are needed for translation to clinical settings. Another hurdle in translating carbon nanotube-based materials for clinical applications is lack of abundant data on nanotube's long-term safety and efficacy. As produced powder carbon nanomaterials, administered at high doses, appear to cause potential adverse health impact and therefore, the powder should be handled carefully with proper safety measures. However, all carbon nanotubes cannot be considered as one material category for their safety assessments.[177] It should be noted that the biological effects of carbon nanotubes mainly depend on the surface functionalization, solubility and size. Without considering these factors, a general conclusion seems illusive. Furthermore, standardization of nanotube characterization in assessments for biological and environmental safety is necessary for clinical translation. Researchers have recently reviewed carbon nanotube characterization methods, their biological effects, and presented their perspectives on gaps in nanometrology techniques for meaningful toxicological and environmental assessments.[165] As mentioned elsewhere, efforts should also focus on evaluating nanotubes safety and efficacy across their entire life-cycle from synthesis to disposal to assess the impact on human health and the environment.

Author contributions

The manuscript was written through contributions of all authors. All authors have given approval to the final version of the manuscript.

Data availability

No primary research results, software or code have been included and no new data were generated or analysed as part of this review.

Conflicts of interest

There are no conflicts of interest to declare.

Acknowledgements

This work was supported by new faculty startup funds from Textile Engineering, Chemistry and Science Department, North Carolina State University.

References

1 N. Yang, X. Chen, T. Ren, P. Zhang and D. Yang, *Sens. Actuators, B*, 2015, **207**, 690–715.
2 S. Kruss, A. J. Hilmer, J. Zhang, N. F. Reuel, B. Mu and M. S. Strano, *Adv. Drug Delivery Rev.*, 2013, **65**, 1933–1950.
3 A. Jain, A. Homayoun, C. W. Bannister and K. Yum, *Biotechnol. J.*, 2015, **10**, 447–459.
4 P. V. Jena, T. V. Galassi, D. Roxbury and D. A. Heller, *ECS J. Solid State Sci. Technol.*, 2017, **6**, M3075–M3077.
5 R. B. Weisman and J. Kono, *Handbook of Carbon Nanomaterials*, World Scientific, 2019, pp. 1–43.
6 M. J. O'Connell, S. M. Bachilo, C. B. Huffman, V. C. Moore, M. S. Strano, E. H. Haroz, K. L. Rialon, P. J. Boul, W. H. Noon, C. Kittrell, J. Ma, R. H. Hauge, B. R. Weisman and R. E. Smalley, *Science*, 2002, **297**, 593–596.
7 R. B. Weisman, S. M. Bachilo and D. Tsyboulski, *Appl. Phys. A*, 2004, **78**, 1111–1116.
8 R. B. Weisman and S. M. Bachilo, *Nano Lett.*, 2003, **3**, 1235–1238.
9 L. Cognet, D. A. Tsyboulski, J. R. Rocha, C. D. Doyle, J. M. Tour and R. B. Weisman, *Science*, 2007, **316**, 1465–1468.
10 W. Cheung and H. He, Carbon Nanotubes: In Vitro and In Vivo Sensing and Imaging, in *Biosensor Nanomaterials*, ed. S. Li, J. Singh, H. Li and I. A. Banerjee, Wiley-VCH Verlag GmbH & Co. KGaA, Weinheim, 2011.
11 U. Resch-Genger, T. Nann, M. Grabolle, S. Cavaliere-Jaricot and R. Nitschke, *Nat. Methods*, 2008, **5**, 763–775.

12 S. Menon, M. R. Mathew, S. Sam, K. Keerthi and K. G. Kumar, *J. Electroanal. Chem.*, 2020, **878**, 114596.
13 A. Yang and F. Yan, *ACS Appl. Electron. Mater.*, 2021, **3**, 53–67.
14 L. Cognet, D. A. Tsyboulski, J. R. Rocha, C. D. Doyle, J. M. Tour and R. B. Weisman, *Science*, 2007, **316**, 1465–1468.
15 A. J. Siitonen, D. A. Tsyboulski, S. M. Bachilo and R. B. Weisman, *Nano Lett.*, 2010, **10**, 1595–1599.
16 C. Manzoni, A. Gambetta, E. Menna, M. Meneghetti, G. Lanzani and G. Cerullo, *Phys. Rev. Lett.*, 2005, **94**, 207401.
17 S. M. Bachilo, M. S. Strano, C. Kittrell, R. H. Hauge, R. E. Smalley and B. R. Weisman, *Science*, 2002, **306**, 2361–2366.
18 S. Diao, J. L. Blackburn, G. Hong, A. L. Antaris, J. Chang, J. Z. Wu, B. Zhang, K. Cheng, C. J. Kuo and H. Dai, *Angew. Chem., Int. Ed.*, 2015, **54**, 14758–14762.
19 G. Hong, S. Diao, J. Chang, A. L. Antaris, C. Chen, B. Zhang, S. Zhao, D. N. Atochin, P. L. Huang, K. I. Andreasson, C. J. Kuo and H. Dai, *Nat. Photonics*, 2016, **8**, 723–730.
20 A. Hendler-Neumark, V. Wulf and G. Bisker, *Mater. Today Bio*, 2021, **12**, 100175.
21 A. Antonucci, J. Kupis-Rozmysłowicz and A. A. Boghossian, *ACS Appl. Mater. Interfaces*, 2017, **9**, 11321–11331, DOI: **10.1021/acsami.7b00810**.
22 J. Pan, F. Li and J. H. Choi, *J. Mater. Chem. B*, 2017, **5**, 6511–6522.
23 C. Farrera, F. Torres Andón and N. Feliu, *ACS Nano*, 2017, **11**, 10637–10643.
24 C. D. Walkey and W. C. W. Chan, *Chem. Soc. Rev.*, 2012, **41**, 2780–2799.
25 P. W. Barone, S. Baik, D. A. Heller and M. S. Strano, *Nat. Mater.*, 2004, **4**, 86–92.
26 V. Georgakilas, K. Kordatos, M. Prato, D. M. Guldi, M. Holzinger and A. Hirsch, *J. Am. Chem. Soc.*, 2002, **124**, 760–761.
27 N. Karousis, N. Tagmatarchis and D. Tasis, *Chem. Rev.*, 2010, **110**, 5366–5397.
28 V. C. Moore, M. S. Strano, E. H. Haroz, R. H. Hauge, R. E. Smalley, J. Schmidt and Y. Talmon, *Nano Lett.*, 2003, **3**, 1379–1382.
29 M. J. O'Connell, P. Boul, L. M. Ericson, C. Huffman, Y. Wang, E. Haroz, C. Kuper, J. Tour, K. D. Ausman and R. E. Smalley, *Chem. Phys. Lett.*, 2001, **342**, 265–271.
30 E. J. Wallace and M. S. P. Sansom, *Nanotechnology*, 2008, **20**, 045101.
31 K. Yurekli, C. A. Mitchell and R. Krishnamoorti, *J. Am. Chem. Soc.*, 2004, **126**, 9902–9903.
32 M. Zheng, A. Jagota, E. D. Semke, B. A. Diner, R. S. Mclean, S. R. Lustig, R. E. Richardson and N. G. Tassi, *Nat. Mater.*, 2003, **2**, 338–342.
33 Y. Wu, J. S. Hudson, Q. Lu, J. M. Moore, A. S. Mount, A. M. Rao, E. Alexov and P. C. Ke, *J. Phys. Chem. B*, 2006, **110**, 2475–2478.
34 H. Wang, S. Michielssens, S. L. C. Moors and A. Ceulemans, *Nano Res.*, 2009, **2**, 945–954.
35 D. Roxbury, S. Zhang, J. Mittal, W. F. Degrado and A. Jagota, *J. Phys. Chem. C*, 2013, **117**, 26255–26261.
36 M. S. Arnold, M. O. Guler, M. C. Hersam and S. I. Stupp, *Langmuir*, 2005, **21**, 4705–4709.
37 K. R. Karnati and Y. Wang, *Phys. Chem. Chem. Phys.*, 2018, **20**, 9389.
38 D. Roxbury, J. Mittal and A. Jagota, *Nano Lett.*, 2012, **12**, 1464–1469.
39 J. Budhathoki-Uprety, P. V. Jena, D. Roxbury and D. A. Heller, *J. Am. Chem. Soc.*, 2014, **136**, 15545–15550.
40 J. Gao, M. A. Loi, E. J. F. de Carvalho and M. C. dos Santos, *ACS Nano*, 2011, **5**, 3993–3999.
41 A. Nish, J. Hwang, J. Doig and R. J. Nicholas, *Nat. Nanotechnol.*, 2007, **2**, 640–646.
42 N. A. Rice and A. Adronov, *Macromolecules*, 2013, **46**, 3850–3860.
43 N. A. Rice, K. Soper, N. Zhou, E. Merschrod and Y. Zhao, *Chem. Commun.*, 2006, 4937–4939.
44 R. Wang, P. Cherukuri, J. G. Duque, T. K. Leeuw, M. K. Lackey, C. H. Moran, V. C. Moore, J. L. Conyers, R. E. Smalley, H. K. Schmidt, R. B. Weisman and P. S. Engel, *Carbon*, 2007, **45**, 2388–2393.
45 M. Bottini, N. Rosato and N. Bottini, *Biomacromolecules*, 2011, **12**, 3381–3393.
46 G. Prencipe, S. M. Tabakman, K. Welsher, Z. Liu, A. P. Goodwin, L. Zhang, J. Henry and H. Dai, *J. Am. Chem. Soc.*, 2009, **131**, 4783–4787.
47 Y. Piao, B. Meany, L. R. Powell, N. Valley, H. Kwon, G. C. Schatz and Y. Wang, *Nat. Chem.*, 2013, **5**, 840–845.
48 A. H. Brozena, M. Kim, L. R. Powell and Y. Wang, *Nat. Rev. Chem.*, 2019, **3**, 375–392.
49 H. Kwon, M. Kim, B. Meany, Y. Piao, L. R. Powell and Y. Wang, *J. Phys. Chem. C*, 2015, **119**, 3733–3739.
50 N. Sultana, H. M. Dewey, A. G. Arellano and J. Budhathoki-Uprety, Understanding the Molecular Assemblies of Single Walled Carbon Nanotubes and Tailoring their Photoluminescence for the Next-Generation Optical Nanosensors, *Chem. Mater.*, 2024, **36**(9), 4034–4053.
51 A. J. Siitonen, D. A. Tsyboulski, S. M. Bachilo and R. B. Weisman, *J. Phys. Chem. Lett.*, 2010, **1**, 2189–2192.
52 J. H. Choi and M. S. Strano, *Appl. Phys. Lett.*, 2007, **90**, 223114.
53 C. A. Silvera-Batista, R. K. Wang, P. Weinberg and K. J. Zeigier, *Phys. Chem. Chem. Phys.*, 2010, **12**, 6990–6998.
54 B. A. Larsen, P. Deria, J. M. Holt, I. N. Stanton, M. J. Heben, M. J. Therien and J. L. Blackburn, *J. Am. Chem. Soc.*, 2012, **134**, 12485–12491.
55 Y. Ohno, S. Iwasaki, Y. Murakami, S. Kishimoto, S. Maruyama and T. Mizutani, *Phys. Status Solidi B*, 2007, **244**, 4002–4005.
56 D. A. Heller, G. W. Pratt, J. Zhang, N. Nair, A. J. Hansborough, A. A. Boghossian, N. F. Reuel,

P. W. Barone and M. S. Strano, *Proc. Natl. Acad. Sci. U. S. A.*, 2011, **108**, 8544–8549.
57 J. Kim, D. A. Heller, H. Jin, P. W. Barone, C. Song, J. Zhang, L. J. Trudel, G. N. Wogan, S. R. Tannenbaum and M. S. Strano, *Nat. Chem.*, 2009, **1**, 473–481.
58 L. Hong, N. Nakashima, Y. Li, H. H. Jia and C. Yang, *Chem. – Asian J.*, 2018, **13**, 210–216.
59 A. J. Lee, X. Wang, L. J. Carlson, J. A. Smyder, B. Loesch, X. Tu, M. Zheng and T. D. Krauss, *Nano Lett.*, 2011, **11**, 1636–1640.
60 M. Zheng and B. A. Diner, *J. Am. Chem. Soc.*, 2004, **126**, 15490–15494.
61 M. J. O'Connell, E. E. Eibergen and S. K. Doorn, *Nat. Mater.*, 2005, **4**, 412–418.
62 T. T. S. Lew, V. B. Koman, K. S. Silmore, J. S. Seo, P. Gordiichuk, S. Kwak, M. Park, M. C. Ang, D. T. Khong, M. A. Lee, M. B. Chan-Park, N. Chua and M. S. Strano, *Nat. Plants*, 2020, **6**, 404–415.
63 S. Kruss, M. P. Landry, E. Vander Ende, B. M. A. Lima, N. F. Reuel, J. Zhang, J. Nelson, B. Mu, A. Hilmer and M. Strano, *J. Am. Chem. Soc.*, 2014, **136**, 713–724.
64 J. Budhathoki-Uprety, J. Shah, J. A. Korsen, A. E. Wayne, T. V. Galassi, J. R. Cohen, J. D. Harvey, P. V. Jena, L. V. Ramanathan, E. A. Jaimes and D. A. Heller, *Nat. Commun.*, 2019, **10**, 1–9.
65 R. M. Williams, C. Lee and D. A. Heller, A Fluorescent Carbon Nanotube Sensor Detects the Metastatic Prostate Cancer Biomarker uPA, *ACS Sens.*, 2018, **3**, 1838–1845.
66 J. D. Harvey, H. A. Baker, M. V. Ortiz, A. Kentsis and D. A. Heller, HIV Detection via a Carbon Nanotube RNA Sensor, *ACS Sens.*, 2019, **4**, 1236–1244.
67 J. D. Harvey, P. V. Jena, H. A. Baker, G. H. Zerze, R. M. Williams, T. V. Galassi, D. Roxbury, J. Mittal and D. A. Heller, *Nat. Biomed. Eng.*, 2017, **1**, 0041.
68 R. L. Pinals, F. Ledesma, D. Yang, N. Navarro, S. Jeong, J. E. Pak, L. Kuo, Y. Chuang, Y. Cheng, H. Sun and M. P. Landry, *Nano Lett.*, 2021, **21**, 2272–2280.
69 R. M. Williams, J. D. Harvey, J. Budhathoki-Uprety and D. A. Heller, Glutathione-S-transferase Fusion Protein Nanosensor, *Nano Lett.*, 2020, **20**, 7287–7295.
70 M. M. Safaee, M. Gravely and D. Roxbury, *Adv. Funct. Mater.*, 2021, **31**, 2006254.
71 P. V. Jena, D. Roxbury, T. V. Galassi, L. Akkari, C. P. Horoszko, D. B. Iaea, J. Budhathoki-Uprety, N. Pipalia, A. S. Haka, J. D. Harvey, J. Mittal, F. R. Maxfield, J. A. Joyce and D. A. Heller, *ACS Nano*, 2017, **11**, 10689–10703.
72 J. D. Harvey, R. M. Williams, K. M. Tully, H. A. Baker, Y. Shamay and D. A. Heller, *Nano Lett.*, 2019, **19**, 4343–4354.
73 H. Wu, R. Nißler, V. Morris, N. Herrmann, P. Hu, S. Jeon, S. Kruss and J. P. Giraldo, *Nano Lett.*, 2020, **20**, 2432–2442.
74 D. Adhya, E. Annuario, M. A. Lancaster, J. Price, S. Baron-cohen and D. P. Srivastava, *J. Neuroendocrinol.*, 2018, **30**, e12547.
75 J. W. Honour, *J. Clin. Res. Pediatr. Endocr.*, 2009, **15**, 209–226.
76 W. L. Miller and R. J. Auchus, *Endocr. Rev.*, 2011, **32**, 81–151.
77 J. P. Del Río, M. I. Alliende, N. Molina, F. G. Serrano, S. Molina and P. Vigil, *Front. Public Health*, 2018, **6**, 141.
78 F. Mauvais-Jarvis, D. J. Clegg and A. L. Hevener, *Endocr. Rev.*, 2013, **34**, 309–338.
79 K. M. Gavin, D. R. Seals, A. E. Silver and K. L. Moreau, *J. Clin. Endocrinol. Metab.*, 2009, **94**, 3513–3520.
80 J. Zhang, M. P. Landry, P. W. Barone, J. Kim, S. Lin, Z. W. Ulissi, D. Lin, B. Mu, A. A. Boghossian, A. J. Hilmer, A. Rwei, A. C. Hinckley, S. Kruss, M. A. Shandell, N. Nair, S. Blake, F. Şen, S. Şen, R. G. Croy, D. Li, K. Yum, J. Ahn, H. Jin, D. A. Heller, J. M. Essigmann, D. Blankschtein and M. S. Strano, *Nat. Nanotechnol.*, 2013, **8**, 959–968.
81 M. A. Lee, S. Wang, X. Jin, N. A. Bakh, F. T. Nguyen, J. Dong, K. S. Silmore, X. Gong, C. Pham, K. K. Jones, S. Muthupalani, G. Bisker, M. Son and M. S. Strano, *Adv. Healthcare Mater.*, 2020, **9**, 2000429.
82 K. Welsher, Z. Liu, D. Daranciang and H. Dai, *Nano Lett.*, 2008, **8**, 586–590.
83 R. M. Williams, C. Lee and D. A. Heller, A Fluorescent Carbon Nanotube Sensor Detects the Metastatic Prostate Cancer Biomarker uPA, *ACS Sens.*, 2018, **3**(9), 1838–1845.
84 R. M. Williams, C. Lee, T. V. Galassi, J. D. Harvey, R. Leicher, M. Sirenko, M. A. Dorso, J. Shah, N. Olvera, F. Dao, D. A. Levine and D. A. Heller, Noninvasive ovarian cancer biomarker detection via an optical nanosensor implant, *Sci. Adv.*, 2018, **4**, eaaq1090.
85 F. Prestinaci, P. Pezzotti and A. Pantosti, Antimicrobial resistance: a global multifaceted phenomenon, *Pathog. Global Health*, 2015, **109**(7), 309–318.
86 R. Nißler, O. Bader, M. Dohmen, S. G. Walter, C. Noll, G. Selvaggio, U. Groß and S. Kruss, Remote near infrared identification of pathogens with multiplexed nanosensors, *Nat. Commun.*, 2020, **11**(1), 5995.
87 V. Shumeiko, Y. Zaken, G. Hidas, Y. Paltiel, G. Bisker and O. Shoseyov, *Peptide-Encapsulated Single-Wall Carbon Nanotube-Based Near-Infrared Optical Nose for Bacteria Detection and Classification*, Institute of Electrical and Electronics Engineers (IEEE), 2022; *IEEE Sens. J.*, 2022, **22**(7), 6277–6287.
88 C. Jiang, G. Wang, R. Hein, N. Liu, X. Luo and J. J. Davis, *Chem. Rev.*, 2020, **120**, 3852–3889, DOI: **10.1021/acs.chemrev.9b00739**.
89 G. Sudhakararao, K. A. Priyadarsini, G. Kiran, P. Karunakar and K. Chegu, Physiological Role of Proteins and their Functions in Human Body, *Int. J. Pharma Res. Health Sci.*, 2019, **7**(1), 2874–2878.
90 N. Rifai, M. A. Gillette and S. A. Carr, Protein biomarker discovery and validation: the long and uncertain path to clinical utility, *Nat. Biotechnol.*, 2006, **24**(8), 971–983.
91 A. Hendler-Neumark and G. Bisker, Fluorescent Single-Walled Carbon Nanotubes for Protein Detection, *Sensors*, 2019, **19**(24), 5403.
92 M. P. Landry, H. Ando, A. Y. Chen, J. Cao, V. I. Kottadiel, L. Chio, D. Yang, J. Dong, T. K. Lu and M. S. Strano,

Single-molecule detection of protein efflux from microorganisms using fluorescent single-walled carbon nanotube sensor arrays, *Nat. Nanotechnol.*, 2017, **12**(4), 368–377.

93 G. Bisker, J. Dong, H. D. Park, N. M. Iverson, J. Ahn, J. T. Nelson, M. P. Landry, S. Kruss and M. S. Strano, Protein-targeted corona phase molecular recognition, *Nat. Commun.*, 2016, **7**, 10241, DOI: **10.1038/ncomms10241**.

94 E. Gerstman, A. Hendler-Neumark, V. Wulf and G. Bisker, Monitoring the Formation of Fibrin Clots as Part of the Coagulation Cascade Using Fluorescent Single-Walled Carbon Nanotubes, *ACS Appl. Mater. Interfaces*, 2023, **15**(18), 21866–21876.

95 X. Jin, M. A. Lee, X. Gong, V. B. Koman, D. J. Lundberg, S. Wang, N. A. Bakh, M. Park, J. I. Dong, D. Kozawa, S. Cho and M. S. Strano, Corona Phase Molecular Recognition of the Interleukin-6 (IL-6) Family of Cytokines Using nIR Fluorescent Single-Walled Carbon Nanotubes, *ACS Appl. Nano Mater.*, 2023, **6**(11), 9791–9804.

96 T. Tanaka, M. Narazaki and T. Kishimoto, IL-6 in Inflammation, Immunity, and Disease, *Cold Spring Harbor Perspect. Biol.*, 2014, **6**(10), a016295.

97 K. K. Kummer, M. Zeidler, T. Kalpachidou and M. Kress, Role of IL-6 in the regulation of neuronal development, survival and function, *Cytokine*, 2021, **144**, 155582.

98 R. Ehrlich, A. Hendler-neumark, V. Wulf, D. Amir and G. Bisker, Optical Nanosensors for Real–Time Feedback on Insulin Secretion by β–Cells, *Small*, 2021, **17**, 2101660.

99 G. Wilcox, Insulin and Insulin resistance, *Clin. Biochem. Rev.*, 2005, **26**(2), 19–39.

100 A. Bascones-Martinez, P. Matesanz-Perez, M. Escribano-Bermejo, M. Gonzalez-Moles, J. Bascones-Ilundain and J. Meurman, Periodontal disease and diabetes-Review of the literature, *Med. Oral. Patol. Oral. Cir. Bucal.*, 2011, **16**(6), e722–e729.

101 G. Bisker, N. A. Bakh, M. A. Lee, J. Ahn, M. Park, E. B. O′connell, N. M. Iverson and M. S. Strano, Insulin Detection Using a Corona Phase Molecular Recognition Site on Single-Walled Carbon Nanotubes, *ACS Sens.*, 2018, **3**(2), 367–377.

102 J. Wang, J. Chen and S. Sen, MicroRNA as Biomarkers and Diagnostics, *J. Cell. Physiol.*, 2016, **231**(1), 25–30.

103 A. Hendler-Neumark, V. Wulf and G. Bisker, Single-Walled Carbon Nanotube Sensor Selection for the Detection of MicroRNA Biomarkers for Acute Myocardial Infarction as a Case Study, *ACS Sens.*, 2023, **8**(10), 3713–3722.

104 R. A. Nixon, The role of autophagy in neurodegenerative disease, *Nat. Med.*, 2013, **19**(8), 983–997.

105 T. Hendrikx, S. M. A. Walenbergh, M. H. Hofker and R. Shiri-sverdlov, Lysosomal cholesterol accumulation: driver on the road to inflammation during atherosclerosis and non–alcoholic steatohepatitis, *Obes. Rev.*, 2014, **15**(5), 424–433.

106 A. H. Futerman and G. Van Meer, The cell biology of lysosomal storage disorders, *Nat. Rev. Mol. Cell Biol.*, 2004, **5**(7), 554–565.

107 T. Kirkegaard and M. Jäättelä, Lysosomal involvement in cell death and cancer, *Biochim. Biophys. Acta*, 2009, **1793**(4), 746–754.

108 T. V. Galassi, M. Antman-Passig, Z. Yaari, J. Jessurun, R. E. Schwartz and D. A. Heller, Long-term in vivo biocompatibility of single-walled carbon nanotubes, *PLoS One*, 2020, **15**(5), e0226791.

109 T. V. Galassi, P. V. Jena, J. Shah, G. Ao, E. Molitor, Y. Bram, A. Frankel, J. Park, J. Jessurun, D. S. Ory, A. Haimovitz-Friedman, D. Roxbury, J. Mittal, M. Zheng, R. E. Schwartz and D. A. Heller, *Sci. Transl. Med.*, 2018, **10**(461), eaar2680.

110 M. Antman-Passig, Z. Yaari, D. Goerzen, R. Parikh, S. Chatman, L. E. Komer, C. Chen, E. Grabarnik, M. Mathieu, A. Haimovitz-Friedman and D. A. Heller, Nanoreporter Identifies Lysosomal Storage Disease Lipid Accumulation Intracranially, *Nano Lett.*, 2023, **23**(23), 10687–10695.

111 J. R. Stone, S. Yang, E. Cadenas, J. Keller, C. K. Sen and J. Yodoi, Hydrogen Peroxide: A Signaling Messenger, *Antioxid. Redox Signaling*, 2006, **8**(3–4), 243–270.

112 Y. Xu, P. E. Pehrsson, L. Chen and W. Zhao, Controllable Redox Reaction of Chemically Purified DNA–Single Walled Carbon Nanotube Hybrids with Hydrogen Peroxide, *J. Am. Chem. Soc.*, 2008, **130**(31), 10054–10055.

113 H. Jin, D. A. Heller, M. Kalbacova, J. Kim, J. Zhang, A. A. Boghossian, N. Maheshri and M. S. Strano, Detection of single-molecule H_2O_2 signalling from epidermal growth factor receptor using fluorescent single-walled carbon nanotube, *Nat. Nanotechnol.*, 2010, **5**(4), 302–309.

114 S. Bhattacharya, X. Gong, E. Wang, S. K. Dutta, J. R. Caplette, M. Son, F. T. Nguyen, M. S. Strano and D. Mukhopadhyay, DNA–SWCNT Biosensors Allow Real-Time Monitoring of Therapeutic Responses in Pancreatic Ductal Adenocarcinoma, *Cancer Res.*, 2019, **79**(17), 4515–4523.

115 D. A. Heller, H. Jin, B. M. Martinez, D. Patel, B. M. Miller, T. Yeung, P. V. Jena, C. Höbartner, T. Ha, S. K. Silverman and M. S. Strano, Multimodal optical sensing and analyte specificity using single-walled carbon nanotubes, *Nat. Nanotechnol.*, 2009, **4**(2), 114–120.

116 P. K. Robinson, Enzymes: principles and biotechnological applications, *Essays Biochem.*, 2015, **59**, 1–41, DOI: **10.1042/bse0590001**. Erratum in: P. K. Robinson, Enzymes: principles and biotechnological applications, *Essays Biochem.*, 2015, **59**, 75.

117 S. Chaturvedi, A. K. Singh, A. K. Keshari, S. Maity, S. Sarkar and S. Saha, Human Metabolic Enzymes Deficiency: A Genetic Mutation Based Approach, *Scientifica*, 2016, **2016**, 9828672.

118 S. Costanzi, J. Machado and M. Mitchell, Nerve Agents: What They Are, How They Work, How to Counter Them, *ACS Chem. Neurosci.*, 2018, **9**(5), 873–885.

119 V. Pozzi, R. Campagna, D. Sartini and M. Emanuelli, Enzymes Dysregulation in Cancer: From Diagnosis to Therapeutical Approaches, *Int. J. Mol. Sci.*, 2023, **24**(18), 13815.

120 S. Basu, A. Hendler-Neumark and G. Bisker, Monitoring Enzyme Activity Using Near-Infrared Fluorescent Single-Walled Carbon Nanotubes, *ACS Sens.*, 2024, **9**(5), 2237–2253.

121 D. Loewenthal, D. Kamber and G. Bisker, Monitoring the Activity and Inhibition of Cholinesterase Enzymes using Single-Walled Carbon Nanotube Fluorescent Sensors, *Anal. Chem.*, 2022, **94**(41), 14223–14231.

122 S. Basu, A. Hendler-neumark and G. Bisker, Rationally Designed Functionalization of Single–Walled Carbon Nanotubes for Real–Time Monitoring of Cholinesterase Activity and Inhibition in Plasma, *Small*, 2024, **20**, 2309481.

123 L. Cohen and D. R. Walt, Highly Sensitive and Multiplexed Protein Measurements, *Chem. Rev.*, 2019, **119**(1), 293–321.

124 X. Zhang, Q. Yang, Y. Lang, X. Jiang and P. Wu, Rationale of 3,3′,5,5′-Tetramethylbenzidine as the Chromogenic Substrate in Colorimetric Analysis, *Anal. Chem.*, 2020, **92**(18), 12400–12406.

125 J. T. Metternich, B. Hill, J. A. C. Wartmann, C. Ma, K. Neutsch, S. Kruss, R. M. Kruskop, S. Herbertz and B. Nanosensors, Signal Amplification and Near-Infrared Translation of Enzymatic Reactions by Nanosensors, *Angew. Chem., Int. Ed.*, 2024, **63**, e202316965.

126 H. Wu, N. Tito and J. P. Giraldo, *ACS Nano*, 2017, **11**, 11283–11297, DOI: **10.1021/acsnano.7b05723**.

127 R. Nißler, A. T. Müller, F. Dohrman, L. Kurth, H. Li, E. G. Cosio, B. S. Flavel, J. P. Giraldo, A. Mithöfer and S. Kruss, Detection and Imaging of the Plant Pathogen Response by Near-Infrared Fluorescent Polyphenol Sensors, *Angew. Chem. Int. Ed.*, 2022, **61**, e202108373.

128 E. H. Colebrook, S. G. Thomas, A. L. Phillips and P. Hedden, The role of gibberellin signalling in plant responses to abiotic stress, *J. Exp. Biol.*, 2014, **217**(Pt 1), 67–75.

129 K. Boonyaves, M. C. Ang, M. Park, J. Cui, D. T. Khong, G. P. Singh, V. B. Koman, X. Gong, T. K. Porter, S. W. Choi, K. Chung, N. Chua, D. Urano and M. S. Strano, Near-Infrared Fluorescent Carbon Nanotube Sensors for the Plant Hormone Family Gibberellins, *Nano Lett.*, 2023, **23**(3), 916–924.

130 V. Wulf, E. Bichachi, A. Hendler-neumark, T. Massarano, A. B. Leshem, A. Lampel and G. Bisker, Multicomponent System of Single–Walled Carbon Nanotubes Functionalized with a Melanin–Inspired Material for Optical Detection and Scavenging of Metals, *Adv. Funct. Mater.*, 2022, **32**, 2209688, DOI: **10.1002/adfm.202209688**.

131 X. Gong, S. Cho, S. Kuo, B. Ogunlade, K. Tso, D. P. Salem and M. S. Strano, Divalent Metal Cation Optical Sensing Using Single-Walled Carbon Nanotube Corona Phase Molecular Recognition, *Anal. Chem.*, 2022, **94**(47), 16393–16401.

132 H. M. Dewey, J. Jones, S. Lucas, S. Hall, N. Sultana, S. M. Abello and J. Budhathoki-Uprety, Carbon Nanotubes for Optical Detection of Quaternary Ammonium Compounds in Complex Media, *ACS Appl. Nano Mater.*, 2023, **6**(17), 15530–15539.

133 K. J. Barnham and A. I. Bush, Biological metals and metal-targeting compounds in major neurodegenerative diseases, *Chem. Soc. Rev.*, 2014, **43**, 6727–6749.

134 Q. Y. Chen, T. Desmarais and M. Costa, Metals and Mechanisms of Carcinogenesis, *Annu. Rev. Pharmacol. Toxicol.*, 2019, **59**, 537–554.

135 H. M. Dewey, J. M. Jones, M. R. Keating and J. Budhathoki-Uprety, *ACS Chem. Health Saf.*, 2022, **29**, 27–38, DOI: **10.1021/acs.chas.1c00026**.

136 W. A. Arnold, A. Blum, J. Branyan, T. A. Bruton, C. C. Carignan, G. Cortopassi, S. Datta, J. Dewitt, A. Doherty, R. U. Halden, H. Harari, E. M. Hartmann, T. C. Hrubec, S. Iyer, C. F. Kwiatkowski, J. Lapier, D. Li, L. Li, J. G. Muñiz Ortiz, A. Salamova, T. Schettler, R. P. Seguin, A. Soehl, R. Sutton, L. Xu and G. Zheng, Quaternary Ammonium Compounds: A Chemical Class of Emerging Concern, *Environ. Sci. Technol.*, 2023, **57**(20), 7645–7665.

137 V. Shumeiko, Y. Paltiel, G. Bisker, Z. Hayouka and O. Shoseyov, A Paper-Based Near-Infrared Optical Biosensor for Quantitative Detection of Protease Activity Using Peptide-Encapsulated SWCNTs, *Sensors*, 2020, **20**(18), 5247.

138 W. Meng, A. Pal, S. M. Bachilo, R. B. Weisman and S. Nagarajaiah, Next-generation 2D optical strain mapping with strain-sensing smart skin compared to digital image correlation, *Sci. Rep.*, 2022, **12**(1), 11226.

139 E. M. Ahmed, Hydrogel: Preparation, characterization, and applications: A review, *J. Adv. Res.*, 2015, **6**(2), 105–121.

140 S. Bashir, M. Hina, J. Iqbal, A. H. Rajpar, M. A. Mujtaba, N. A. Alghamdi, S. Wageh, K. Ramesh and S. Ramesh, Fundamental Concepts of Hydrogels: Synthesis, Properties, and Their Applications, *Polymers*, 2020, **12**(11), 2702.

141 B. K. Mann, A. S. Gobin, A. T. Tsai, R. H. Schmedlen and J. L. West, Smooth muscle cell growth in photopolymerized hydrogels with cell adhesive and proteolytically degradable domains: synthetic ECM analogs for tissue engineering, *Biomaterials*, 2001, **22**(22), 3045–3051.

142 M. C. Ford, J. P. Bertram, S. R. Hynes, M. Michaud, Q. Li, M. Young, S. S. Segal, J. A. Madri, E. B. Lavik and R. Langer, A macroporous hydrogel for the coculture of neural progenitor and endothelial cells to form functional vascular networks in vivo, *Proc. Natl. Acad. Sci. U. S. A.*, 2006, **103**(8), 2512–2517.

143 P. W. Barone, H. Yoon, R. Ortiz-García, J. Zhang, J. Ahn, J. Kim and M. S. Strano, Modulation of Single-Walled Carbon Nanotube Photoluminescence by Hydrogel Swelling, *ACS Nano*, 2009, **3**(12), 3869–3877.

144 N. M. Iverson, G. Bisker, E. Farias, V. Ivanov, J. Ahn, G. N. Wogan and M. S. Strano, Quantitative Tissue Spectroscopy of Near Infrared Fluorescent Nanosensor Implants, *J. Biomed. Nanotechnol.*, 2016, **12**(5), 1035–1047.

145 Z. Cohen, D. J. Alpert, A. C. Weisel, A. Roach, S. Rahman, P. V. Gaikwad, S. B. Nicoll and R. M. Williams, Noninvasive Injectable Optical Nanosensor-Hydrogel Hybrids Detect Doxorubicin in Living Mice, *Adv. Opt. Mater.*, 2024, **12**, 2303324.

146 R. Nißler, O. Bader, M. Dohmen, S. G. Walter, C. Noll, G. Selvaggio, U. Groß and S. Kruss, *Nat. Commun.*, 2020, **11**, 5995, DOI: **10.1038/s41467-020-19718-5**.

147 H. Park, B. Choi, J. Hu and M. Lee, Injectable chitosan hyaluronic acid hydrogels for cartilage tissue engineering, *Acta Biomater.*, 2013, **9**(1), 4779–4786, DOI: **10.1016/j.actbio.2012.08.033**.

148 A. T. Rowley, R. R. Nagalla, S. Wang and W. F. Liu, Extracellular Matrix–Based Strategies for Immunomodulatory Biomaterials Engineering, *Adv. Healthcare Mater.*, 2019, **8**(8), e1801578, DOI: **10.1002/adhm.201801578**.

149 V. Wulf and G. Bisker, Single-Walled Carbon Nanotubes as Fluorescent Probes for Monitoring the Self-Assembly and Morphology of Peptide/Polymer Hybrid Hydrogels, *Nano Lett.*, 2022, **22**(22), 9205–9214.

150 M. A. Lee, X. Jin, S. Muthupalani, N. A. Bakh, X. Gong and M. S. Strano, In vivo fluorescent nanosensor implants based on hydrogel-encapsulation: investigating the inflammation and the foreign-body response, *J. Nanobiotechnol.*, 2023, **21**, 133.

151 A. Spreinat, M. M. Dohmen, J. Lüttgens, N. Herrmann, L. F. Klepzig, R. Nißler, S. Weber, F. A. Mann, J. Lauth and S. Kruss, Quantum Defects in Fluorescent Carbon Nanotubes for Sensing and Mechanistic Studies, *J. Phys. Chem. C*, 2021, **125**(33), 18341–18351.

152 T. Shiraki, H. Onitsuka, T. Shiraishi and N. Nakashima, *Chem. Commun.*, 2016, **52**, 12972, DOI: **10.1039/c6cc07287a**.

153 J. T. Metternich, J. A. C. Wartmann, L. Sistemich, R. Nißler, S. Herbertz and S. Kruss, Near-Infrared Fluorescent Biosensors Based on Covalent DNA Anchors, *J. Am. Chem. Soc.*, 2023, **145**(27), 14776–14783.

154 Y. Niidome, R. Wakabayashi, M. Goto, T. Fujigaya and T. Shiraki, *Nanoscale*, 2022, **14**, 13090, DOI: **10.1039/d2nr01440h**.

155 Y. Niidome, R. Hamano, K. Nakamura, S. Qi, S. Ito, B. Yu, Y. Nagai, N. Tanaka, T. Mori, Y. Katayama, T. Fujigaya and T. Shiraki, Near-infrared photoluminescent detection of serum albumin using single-walled carbon nanotubes locally functionalized with a long-chain fatty acid, *Carbon*, 2024, **216**, 118533.

156 P. Galonska, J. M. Mohr, C. A. Schrage, L. Schnitzler and S. Kruss, Guanine Quantum Defects in Carbon Nanotubes for Biosensing, *J. Phys. Chem. Lett.*, 2023, **14**(14), 3483–3490.

157 Z. Yaari, Y. Yang, E. Apfelbaum, C. Cupo, A. H. Settle, Q. Cullen, W. Cai, K. L. Roche, D. A. Levine, M. Fleisher, L. Ramanathan, M. Zheng, A. Jagota and D. A. Heller, A perception-based nanosensor platform to detect cancer biomarkers, *Sci. Adv.*, 2021, 7(47), eabj0852, DOI: **10.1126/sciadv.abj0852**.

158 Z. A. De Los Santos, Z. Lin and M. Zheng, Optical Detection of Stereoselective Interactions with DNA-Wrapped Single-Wall Carbon Nanotubes, *J. Am. Chem. Soc.*, 2021, **143**(49), 20628–20632.

159 M. Kim, C. Chen, P. Wang, J. J. Mulvey, Y. Yang, C. Wun, M. Antman-Passig, H. Luo, S. Cho, K. Long-Roche, L. V. Ramanathan, A. Jagota, M. Zheng, Y. Wang and D. A. Heller, Detection of ovarian cancer via the spectral fingerprinting of quantum-defect-modified carbon nanotubes in serum by machine learning, *Nat. Biomed. Eng.*, 2022, **6**(3), 267–275.

160 X. Gong, N. Renegar, R. Levi and M. S. Strano, Machine learning for the discovery of molecular recognition based on single-walled carbon nanotube corona-phases, *npj Comput. Mater.*, 2022, **8**, 135, DOI: **10.1038/s41524-022-00795-7**.

161 P. Kelich, S. Jeong, N. Navarro, J. Adams, X. Sun, H. Zhao, M. P. Landry and L. Vuković, Discovery of DNA–Carbon Nanotube Sensors for Serotonin with Machine Learning and Near-infrared Fluorescence Spectroscopy, *ACS Nano*, 2022, **16**(1), 736–745.

162 F. Yang, M. Wang, D. Zhang, J. Yang, M. Zheng and Y. Li, *Chem. Rev.*, 2020, **120**, 2693–2758, DOI: **10.1021/acs.chemrev.9b00835**.

163 T. N. Krabach, C. O. Staller, S. N. Dejewski, T. J. Cunningham, M. Herring and E. R. Fossum, *InGaAs detectors for miniature infrared instruments, Infrared and Millimeter-Wave Engineering*, SPIE, 1993, vol. 1874.

164 H. Heidari-Bafroui, B. Ribeiro, A. Charbaji, C. Anagnostopoulos and M. Faghri, *Measurement*, 2021, **173**, 108607, DOI: **10.1016/j.measurement.2020.108607**.

165 M. Kim, D. Goerzen, P. V. Jena, E. Zeng, M. Pasquali, R. A. Meidl and D. A. Heller, *Nat. Rev. Mater.*, 2024, **9**, 63–81, DOI: **10.1038/s41578-023-00611-8**.

166 C. Liu, Y. Liu, Y. Zhang, R. Wei and H. Zhang, Tandem extraction strategy for separation of metallic and semiconducting SWCNTs using condensed benzenoid molecules: effects of molecular morphology and solvent, *Phys. Chem. Chem. Phys.*, 2009, **11**, 7257–7267.

167 R. B. Weisman, S. M. Bachilo and D. Tsyboulski, *Appl. Phys. A*, 2004, **78**, 1111–1116.

168 J. Budhathoki-Uprety, R. E. Langenbacher, P. V. Jena, D. Roxbury and D. A. Heller, A Carbon Nanotube Optical Sensor Reports Nuclear Entry via a Noncanonical Pathway, *ACS Nano*, 2017, **11**(4), 3875–3882.

169 S. Lin and D. Blankschtein, Role of the Bile Salt Surfactant Sodium Cholate in Enhancing the Aqueous Dispersion Stability of Single-Walled Carbon Nanotubes: A Molecular Dynamics Simulation Study, *J. Phys. Chem. B*, 2010, **114**(47), 15616–15625.

170 N. R. Tummala, B. H. Morrow, D. E. Resasco and A. Striolo, Stabilization of Aqueous Carbon Nanotube Dispersions Using Surfactants: Insights from Molecular Dynamics Simulations, *ACS Nano*, 2010, **4**(12), 7193–7204.

171 L. Li, Q. Cao, H. Liu, X. Qiao, Z. Gu, Y. Yu and C. Zuo, Understanding interactions between poly(styrene–co–

sodium styrene sulfonate) and single–walled carbon nanotubes, *J. Polym. Sci.*, 2021, **59**, 182–190, DOI: **10.1002/pol.20200557**.

172 H. Yang, V. Bezugly, J. Kunstmann, A. Filoramo and G. Cuniberti, Diameter-Selective Dispersion of Carbon Nanotubes via Polymers: A Competition between Adsorption and Bundling, *ACS Nano*, 2015, **9**(9), 9012–9019.

173 J. D. Harvey, G. H. Zerze, K. M. Tully, J. Mittal and D. A. Heller, Electrostatic Screening Modulates Analyte Binding and Emission of Carbon Nanotubes, *J. Phys. Chem. C*, 2018, **122**(19), 10592–10599.

174 N. Sultana, H. Dewey and J. Budhathoki-Uprety, Optical detection of pH changes in artificial sweat using near-infrared fluorescent nanomaterials, *Sens. Diagn.*, 2022, **1**, 1189–1197.

175 J. D. Harvey, H. A. Baker, E. Mercer, J. Budhathoki-Uprety and D. A. Heller, Control of Carbon Nanotube Solvatochromic Response to Chemotherapeutic Agents, *ACS Appl. Mater. Interfaces*, 2017, **9**(43), 37947–37953.

176 H. M. Dewey, N. Mahmood, S. M. Abello, N. Sultana, J. Jones, J. M. Gluck and J. Budhathoki-Uprety, Development of Optical Nanosensors for Detection of Potassium Ions and Assessment of Their Biocompatibility with Corneal Epithelial Cells, *ACS Omega*, 2024, **9**(25), 27338–27348.

177 D. A. Heller, P. V. Jena, M. Pasquali, *et al.*, Banning carbon nanotubes would be scientifically unjustified and damaging to innovation, *Nat. Nanotechnol.*, 2020, **15**, 164–166.